FLUIDIC TEMPERATURE CONTROL SYSTEM

FOR LIQUID-COOLED SPACE SUITS

12128-FR1

September 1969

Prepared under Contract No. NAS 9-8249

by
HONEYWELL INC.
Systems & Research Division
Minneapolis, Minn

for

NATIONAL AERONAUTICS AND SPACE ADMINISTRATION

NASA CR 108330

FLUIDIC TEMPERATURE CONTROL SYSTEM FOR LIQUID-COOLED SPACE SUITS

By J.B. Starr
G. L. Merrill

Distribution of this report is provided in the interest of information exchange. Responsibility for the contents resides in the author or organization that prepared it.

September 1969

FOREWORD

This report documents work performed during a 14-month study and development effort by Honeywell Inc. Systems and Research Center under NASA Contract NAS 9-8243, "Fluidic Temperature Control System for Liquid-Cooled Space Suits." The authors wish to acknowledge the guidance and contributions given this program by the technical monitor, Mr. J. Travis Brown, NASA Manned Spacecraft Center, Houston Texas.

CONTENTS

List of Illustrations

FLUIDIC TEMPERATURE CONTROL SYSTEM
FOR LIQUID-COOLED SPACE SUITS

By James B. Starr and Glenn L. Merrill
Honeywell Inc.

SUMMARY

The purpose of the program was to develop a control system that would modulate coolant temperature at the inlet of a liquid-cooled garment connected to a spacecraft by an umbilical. This was to be accomplished without the addition of electrical or hydraulic signal lines; rather, signals were to be transmitted via already existing liquid supply and return conduits.

The system developed modulates coolant temperature in response to changes in pressure drop across the liquid-cooled garment. Modulation is accomplished within a fluidic temperature controller that would be located in the spacecraft. The controller contains no moving parts, and responds to pressure difference signals of less than 0.1 inch of water. The principal mode considered was manual. Automatic control was considered as an aid in maintaining an acceptable thermal state during complex work situations.

Manual operation of the system proved successful. A special manual-control circuit located at the liquid-cooled garment provides for selection of any one of three levels of cooling. Cooling level adjustment is achieved through a combination of inlet temperature and garment flow rate modulation. Flow rate modulation is needed to provide maximum subject comfort at low metabolic rates. Further improvements in the fluidic mixing valve used in the controller would facilitate control entirely by inlet temperature modulation.

Automatic operation of the system was shown feasible; however, additional development will be required to achieve satisfactory operational characteristics . Automatic operation is obtained by using sensors that produce an effective orifice area variation with skin tmeperature variations. Preliminary analysis had indicated that four sensors of a type developed under a previous study would be adequate if sufficient controller gain could be provided. However, instabilities related to thermal transients necessitated a gain reduction which resulted in marginal system response in the automatic mode. In addition, the process of pretuning the system to the correct pressure-difference-signal band was found to be somewhat awkward.

INTRODUCTION

Utilization of liquid-cooled garments for space flight applications has increased in recent years, stimulated in part by the advantages that liquid-cooled garments exhibit over gas-cooled garments. Liquid-cooled garments can remove heat at a much higher rate while, at the same time, suppressing perspiration. These advantages arise from the existence of conductive and convective heat transfer in liquid-cooled garments as opposed to the limited heat transfer due to evaporation in gas-cooled garments.

Utilization of a liquid-cooled system for control of an astronaut's thermal environment requires that the cooling rate be adjusted to match his metabolic rate. Two basic approaches to cooling rate modulation can be taken: (1) flow-rate modulation while maintaining a fixed nominal liquid inlet temperature; (2) coolant inlet-temperature modulation while maintaining a fixed nominal flow rate.

Flow-rate modulation achieves variations in cooling rate by adjusting the coolant temperature rise in the garment. A reduced flow rate results in a higher temperature rise and a smaller mean temperature difference between the subject's skin and the coolant; hence, a low cooling rate is achieved at low flow rates and vice versa. This method is advantageous from the point of view of system simplicity. That is, cooling rates can be adjusted by a manual control valve located on the garment. The only connections required between the garment and the liquid pumping and cooling equipment are the coolant supply and return lines. The disadvantage of the flow-rate modulation method is that inlet temperature is constant and, at low cooling rates, is a source of discomfort.

Coolant inlet-temperature modulation is thus required for maximum subject comfort. To accomplish this would normally require three liquid conduits connecting the garment to cooling and pumping equipment. Warm and cold fluid supplied by separate conduits could then be mixed at the garment inlet in the proportions required to obtain the desired coolant inlet temperature. A third conduit would return coolant from the garment exit to the pumping and cooling system. However, the use of three rather than two liquid lines within the umbilical for EVA would complicate an already difficult packaging problem. Continual mixing of warm and cold streams would require a heat source for regeneration of a warm stream; this additional heating would be reflected in a substantially greater load on the spacecraft water cooling system.

A preferred approach to coolant inlet temperature modulation is to locate a liquid temperature controller in the spacecraft. With such a system, signals calling for coolant temperature modulations are transmitted by some means from the astronaut via the umbilical to the controller.

The system discussed in this report centers around the concept of using the already existing supply and return conduits to transmit the control signals.

Control signals are produced by varying the flow resistance across the liquid-cooled garment. These variations can be produced manually by the astronaut through the turning of a valve, or automatically by skin temperature sensors. Fluidic techniques are employed in the coolant temperature controller because of inherent reliability (no moving parts are required) and low signal thresholds that are characteristic of fluidic devices. Nomenclature used in the discussion is defined in Appendix B.

CONTROL CIRCUIT CONCEPT

A control circuit for liquid-cooled aircraft flight suits that facilitates coolant temperature modulation is described in Reference 1. The circuit uses heat rejection from the subject to generate a source of warm water, thus minimizing loads on the water cooling system. The adaptation of that system to an astronaut cooling system is illustrated in Figure 1. The circuit consists basically of two flow loops. One loop includes the liquid-cooled garment (LCG) and the other a heat exchanger (HEX) for liquid cooling. If no fluid flows from the HEX loop to the LCG loop, then water that exits from the liquid-cooled garment is recirculated and, in theory, its temperature will approach that of the skin of the astronaut. This would correspond to a zero-cooling-rate situation. An increase in cooling rate is produced by allowing liquid to flow from the HEX loop into the LCG loop. Maximum cooling is obtained, of course, when the crossover flow between the loops is equal to the flow through the heat exchanger.

Control signals which drive the temperature controller are produced within a fluid circuit that is, in essence, a wheatstone bridge. The umbilical, the liquid-cooled garment, and resistors representing either manually controlled valves or skin temperature sensors, constitute a "garment circuit" which makes up one leg of the bridge. Resistances R_1, R_2, and R_3 form, respectively, the remaining three legs of the bridge. R_3 is made adjustable in order to compensate for changes in umbilical flow resistance; i.e., the system is readily adaptable to a wide range of umbilical lengths. A change in cooling rate can be produced by varying a resistance located in the garment circuit.

As seen in Figure 1, the system requires two circulating pumps. From the viewpoint of system complexity, the necessity of two pumps would appear to be a disadvantage. However, the utilization of two pumps offers a degree of redundancy in the system that is desirable in achieving high reliability. In the event of one pump failure, automatic or manual sequencing could be employed to provide an emergency mode for control of cooling rates. In this emergency mode, one or the other of the two pumps would circulate fluid from the heat exchanger directly to the liquid-cooled garment. The astronaut could then adjust his cooling rate by manually modulating flow rate through the liquid-cooled garment.

GARMENT PRESSURE-DROP CHARACTERISTICS

The design of this system requires a thorough knowledge of the pressure-drop characteristics of the liquid-cooled garment, i.e., it is necessary to know how the garment pressure drop is affected by inlet pressure, temperature, flow rate, and subject position. This knowledge was obtained through experimentation.

Figures 2 through 4 present experimental pressure-drop data for three inlet pressures and three inlet temperatures. The pressure drop varies non-linearly with flow rate and is affected significantly by both inlet pressure and temperature. The extent of this variation is apparent from the crossplot shown in Figure 5. The data reveal that a 40°F change in inlet temperature varies garment pressure drop by nearly 1 psi. This change is attributed to the reduction in liquid viscosity as temperature increases. Increasing inlet gauge pressure also reduces pressure drop through the garment; this is attributed to tube swelling with increasing gauge pressure.

The variation of garment flow resistance with temperature could introduce undesirable transists into the control system. This effect can be offset by designing resistance R_1 (Figure 1) to exhibit a temperature dependence similar to that of the liquid-cooled garment. A fluid resistance that consists of capillary elements, wherein there is laminar flow, in series with a thin-plate orifice can be designed to produce the desired temperature dependence.

Tests were also conducted to determine the effect of subject position on garment pressure drop. As evidenced in Figure 6, various positions produce negligible changes in pressure-drop characteristic.

CONTROLLER DESIGN

The basic function of the fluidic temperature controller is to vary the ratio of warm fluid to cold fluid flowing to the liquid-cooled garment. This modulation must be carried out in response to relatively small pressure difference signals generated within the bridge circuit (shown in Figure 1). The controller must accept the pressure signals at a level that is established by the bridge design, and then amplify them to the magnitude required to modulate the mixture ratio of warm and cold fluid.

The modulation of mixture ratio within the fluidic controller should produce no significant changes in flow impedance in the circuit. This requirement is imposed because of the use of positive displacement pumps in spacecraft water circulating systems. If significant changes and flow impedance did occur within the fluidic controller, then temperature modulation would be accompanied by relatively large changes in pressure levels within the circuit. In general, this would greatly complicate the task of transmitting pressure signals from the bridge circuit to elements within the fluidic temperature controller.
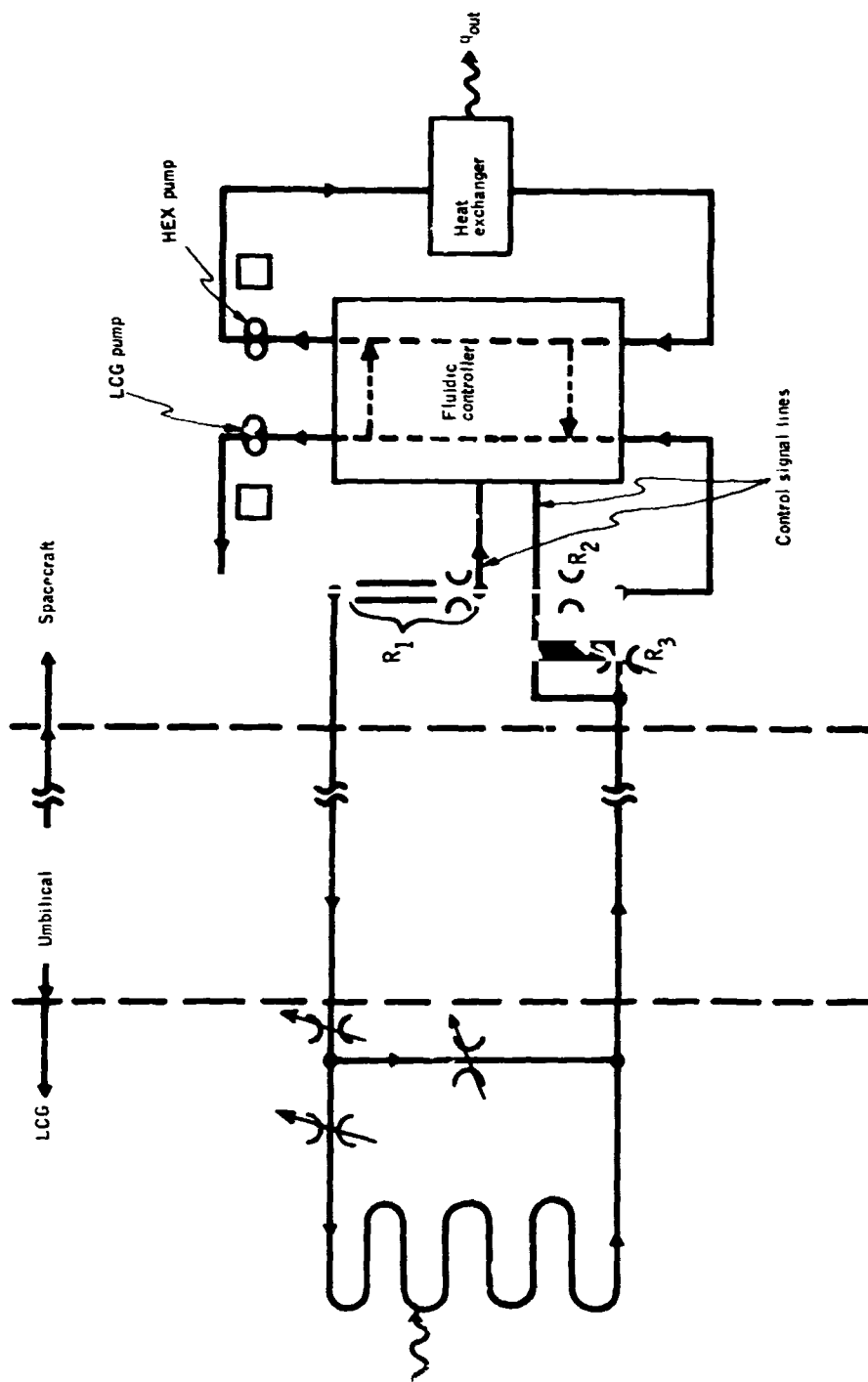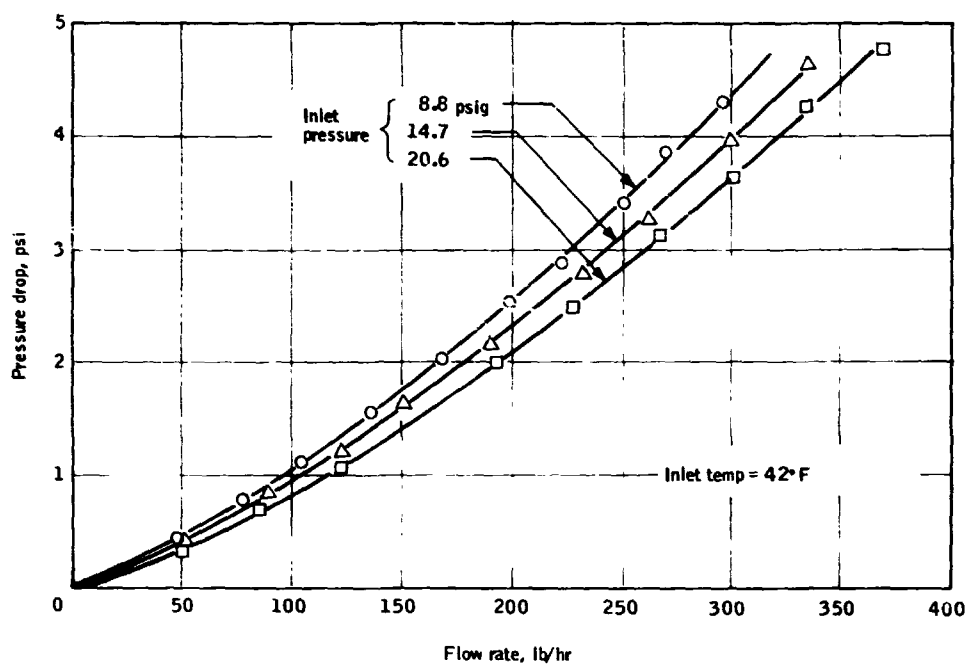
4

Figure 1. Control Circuit Concept

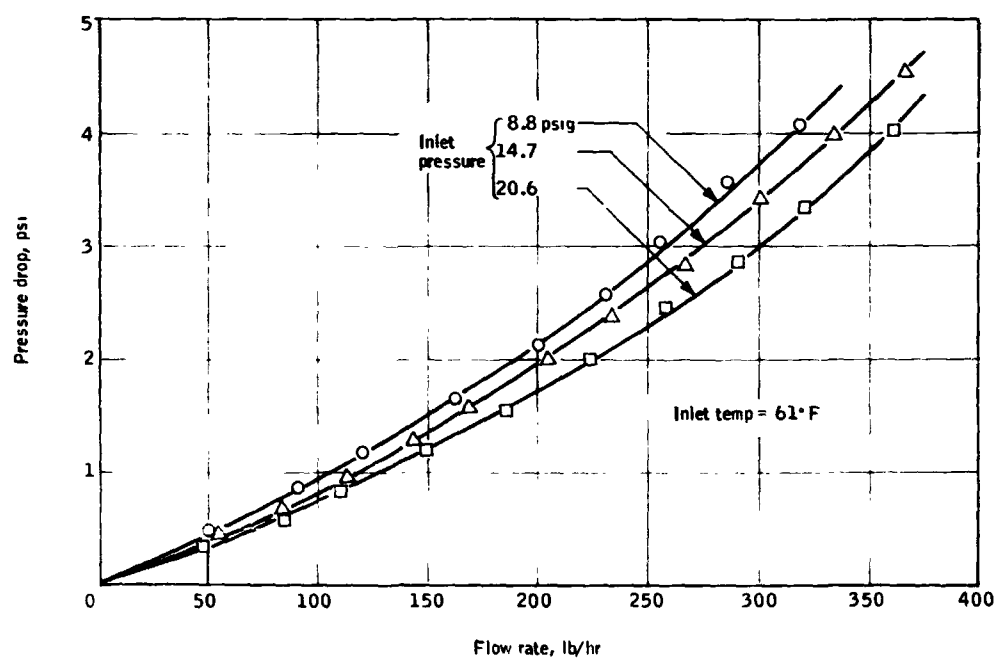Figure 2. Garment Pressure Drop; Inlet Temperature = 42°F

Figure 3. Garment Pressure Drop; Inlet Temperature = 61°F

6
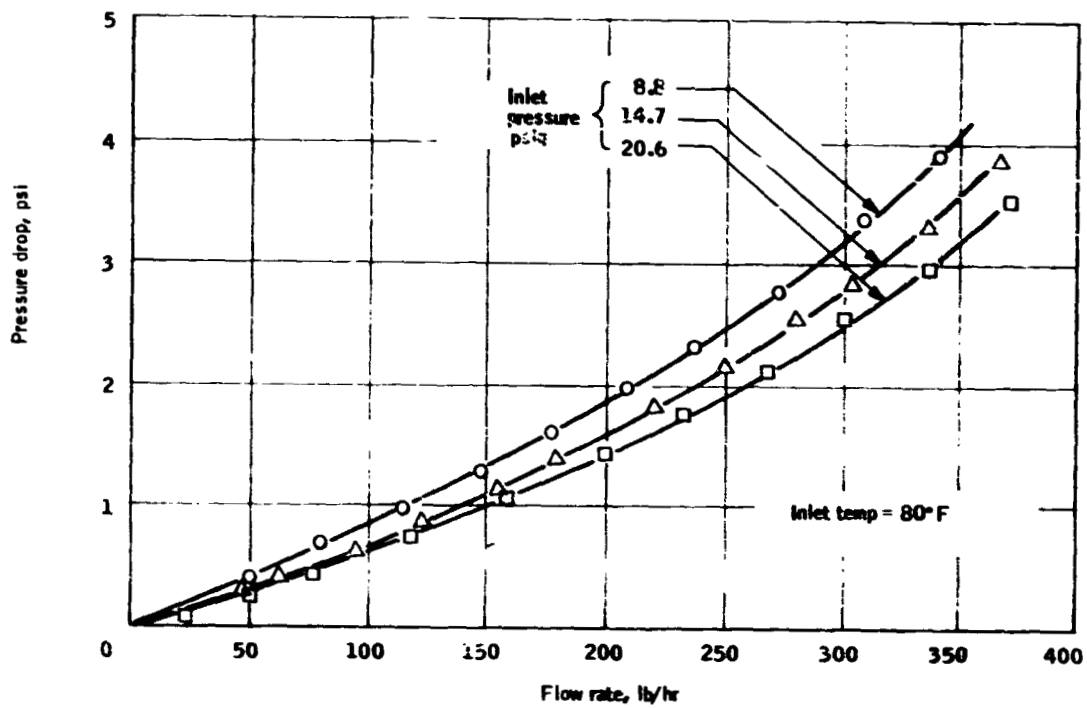
Figure 4. Garment Pressure Drop; Inlet Temperature 80°F
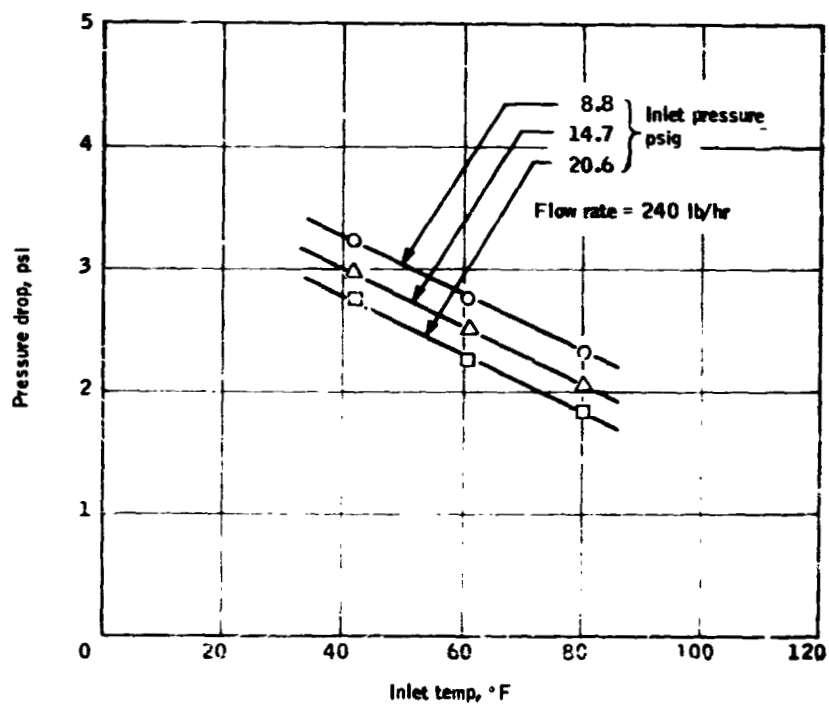
Figure 5. Effect of Pressure Level and Inlet Temperature
on Garment Pressure Drop
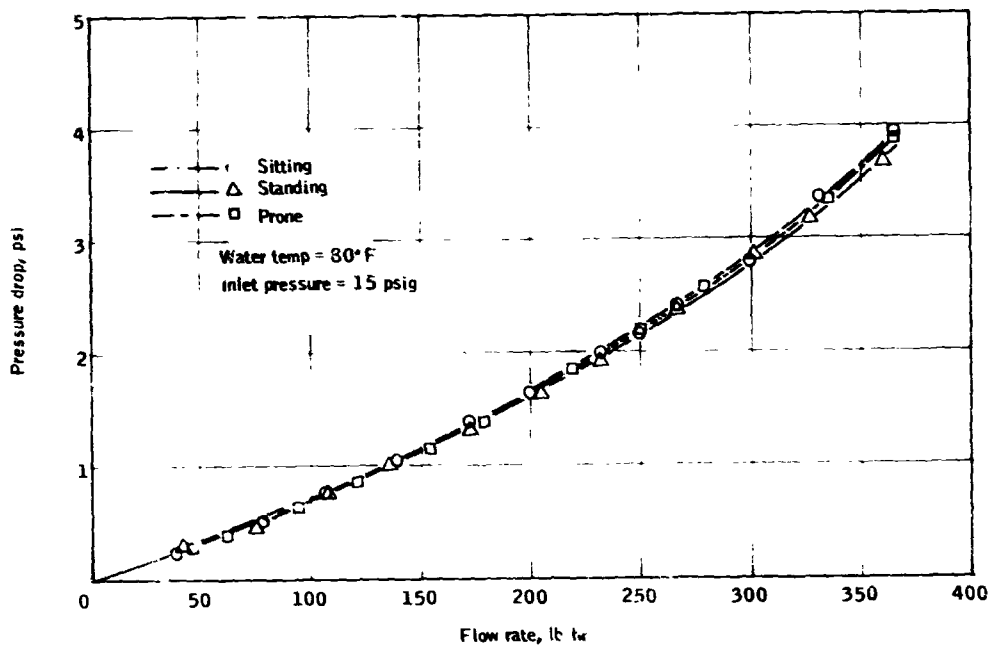
Figure 6. Garment Pressure Drop for Various
Subject Positions

The relationship between cooling rate and mixture ratio produced by the con-
troller is illustrated in Figure 7. This curve was generated from equations in
Appendix A for the case where all of the water in the LCG loop circulates
through the LCG (i.e., γ = 1). The curve shows that for small fractions of
cool fluid circulated from the HEX loop into the LCG loop, substantial cooling
can be produced. For example, a flow fraction of only 0.10 produces a cooling
rate of 700 btu per hour. The controller must therefore be capable of pro-
ducing low mixture ratios to limit cooling at low work rates. Relatively high
cooling rates can be achieved with moderate mixture ratios. For example, a
mixture ratio of only 0.5 produces a cooling rate of 1700 btu per hour. Even
so, mixture ratios approaching 1.0 are desired so that cooling capability of
the LCG system is not to be limited by the controller.

8
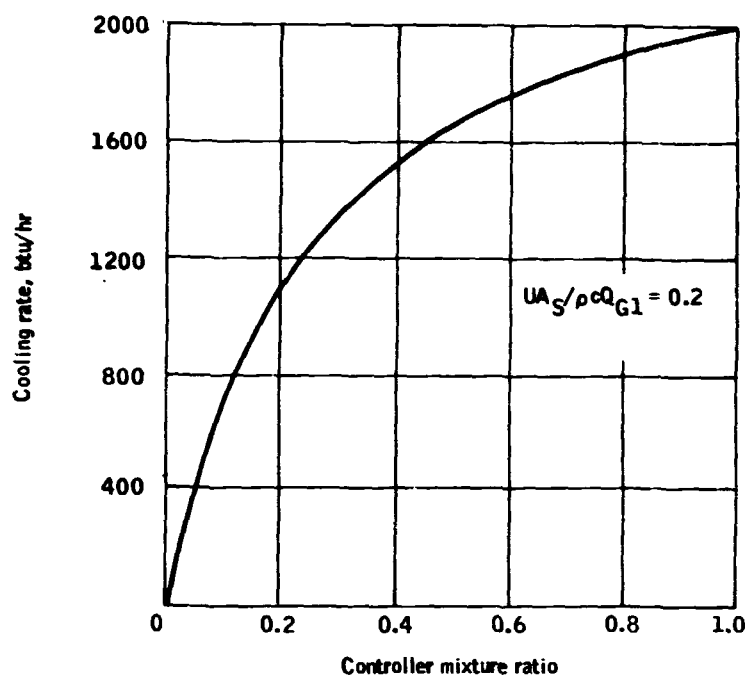
Figure 7. Effect of Controller Mixture Ratio
on Garment Cooling Rate

Fluidic Mixing Valves

The key element in the controller is the fluidic mixing valve. Within this element flows are modulated, without the use of moving parts, to produce the desired mixing of warm and cold streams.

Three basic fluidic devices were considered as candidates for carrying out the mixing function. They were, as shown in Figures 8 through 10, the differential vortex valve, the jet deflection amplifier, and an impact flow modulator.

The differential vortex valve operates on the principle of using jet deflection to divert fluid along either a low-impedance or a high-impedance path. As shown in Figure 8, deflection of the jet to the right causes fluid to enter the vortex chamber along a low-impedance radial path, whereas deflection to the left produces a high-impedance vortical flow path. Vortex valves can produce significant flow modulation; however, the variable impedance inherent in the device makes utilization difficult in constant-flow circuits.

9
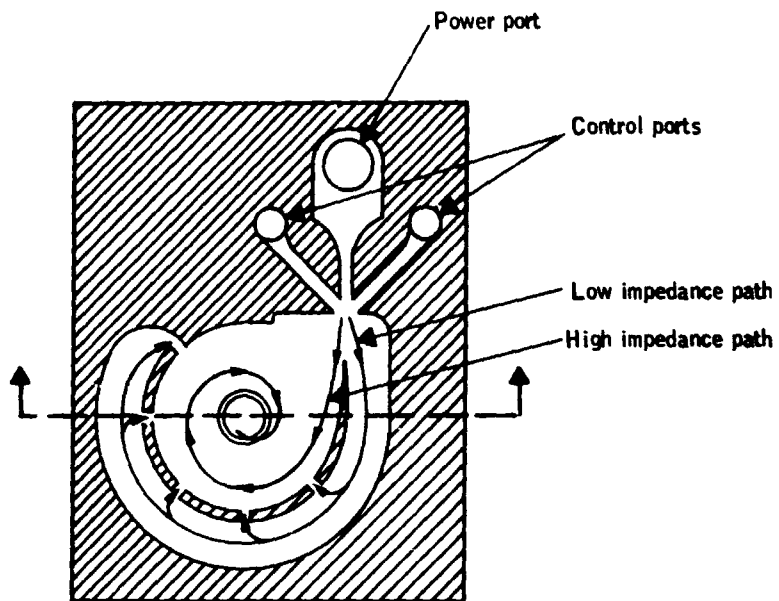
Figure 8. Differential Vortex Valve
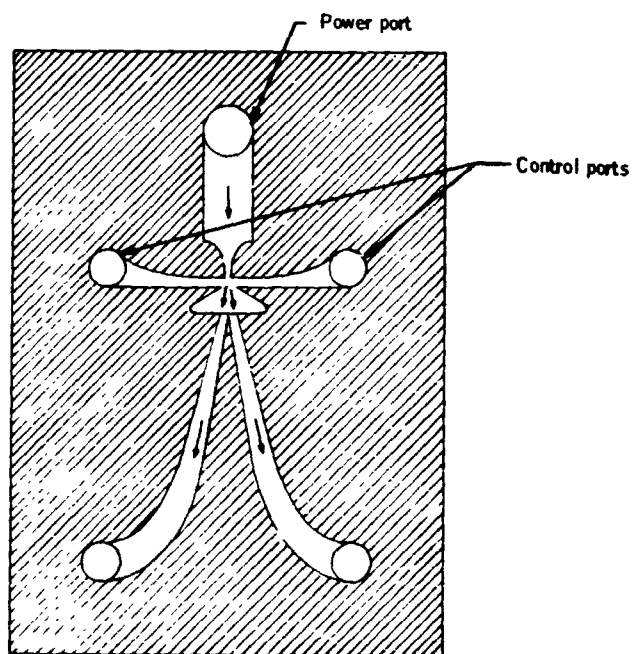
Figure 9. Jet Deflection Amplifier
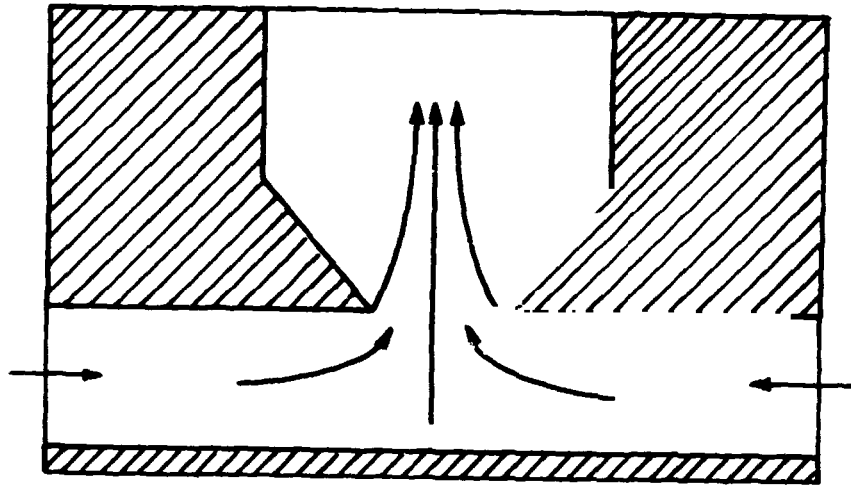
Figure 10. Impact Flow Modulator

The jet-deflection amplifier in Figure 9 diverts flow into either its left or the right outlet branch in response to deflection of a power jet. The advantage of this technique is that flow diverting is produced with no overall impedance change within the device. However, complete capture of the stream into one or the other of the output branches, in theory, requires relatively high velocities for the power jet, and careful matching of the device geometry to downstream flow resistances.

Figure 10 illustrates an impact flow modulator. This device is basically passive in that it reacts only to the pressures of the streams to be mixed. If the pressure of the stream entering from the left is greater than that from the right, then the flow from the left will be substantially greater. In fact, with moderate relative pressure differences, one or the other of the two incoming flows can be reduced to zero.

The mixing valve concept that has evolved from consideration of these fluidic elements makes use of the jet-deflection amplifier and the impact flow modulator. The idea is to use jet deflection amplifiers to produce moderate pressure differences at the inlets of impact flow modulators. The modulators can, in turn, generate substantial changes in mixture ratio.

Figure 11 illustrates the first implementation of the foregoing concept, designated here as Model I. Model I is, in essence, a proportional jet deflection amplifier with impact flow modulators built into each of its two output legs.

Figure 11. Fluidic Mixing Valve; Model I

The impact flow modulators vary mixture ratio as a result of power jet deflection. This deflection arises from varying pressures P_{C1} and P_{C2} at the mixing valve control ports. When P_{C1} is greater than P_{C2}, Q_{CG} is greater than Q_{HG}, and a relatively cool stream flows out of the left-hand output port. At the same time $Q_{CR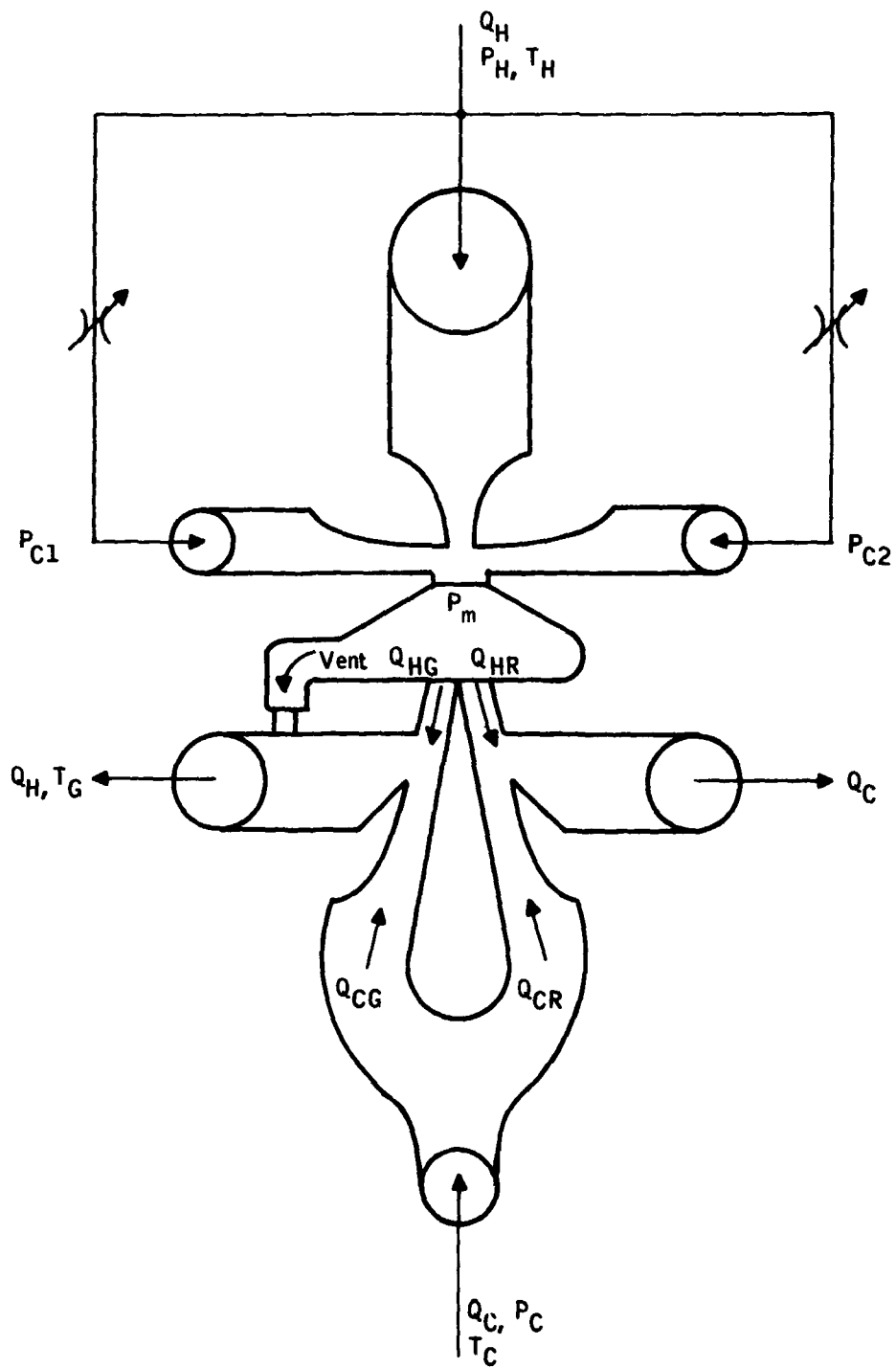}$ is less than Q_{HR}, and the flow out of the right-hand output port is relatively warm. The reverse situation occurs if P_{C2} is greater than P_{C1}. This device is basically a flow diverter rather than a flow throttling device, as is a vortex valve. Consequently, nearly constant impedance to both warm and cold flows is achieved.

Model I was designed, fabricated and tested. Experiments conducted on the mixing valve demonstrated its ability to vary the mixture ratio Q_{CG}/Q_H from zero to 0.58. The data are illustrated in Figure 12 and, according to Figure 7, indicate that cooling rates could be varied from zero to 1800 btu/hr.

Model I possesses several advantages, but limits cooling capacity of the system. The primary advantage is that no control signals need to be transmitted to the HEX loop of the liquid-cooled garment. Control signals originate in the LCG loop; hence, transmission to the HEX loop would result in some residual mixing of warm and cold fluid. This would accentuate the problem of achieving cooling rates low enough to produce comfort at rest conditions. The disadvantage of Model I is that cooling rates are limited to 1800 btu/hr because the maximum obtainable value of Q_{CG}/Q_H is 0.58. If at all possible, a cooling rate of 2000 but/hr should be achievable in order to avoid possible marginal cooling conditions. If cooling rates of less than 1800 but/hr were acceptable, then Model I would be a satisfactory mixing valve.

To achieve higher cooling rates, a second fluidic mixing valve, designated Model II, was designed and fabricated so that a larger range of mixture ratios could be obtained. The Model II design is illustrated in Figure 13. Note that both the cold-supply and warm-supply streams are diverted by control flows, whereas in the Model I design only the warm-supply stream was diverted by control flows. Referring to Figure 13 increasing P_{C1} diverts more warm and less cold fluid into the liquid-cooled garment; conversely, increasing P_{C2} diverts more cold and less warm fluid to the liquid-cooled garment.

The ability of Model II to modulate flow rate ratios is illustrated by the experimental data in Figure 14. Because all mixing occurs within the device itself, determination of mixture ratios from flow rate measurements is not possible. Consequently, one has to resort to temperature measurements to deduce flow rate ratios generated by the fluidic mixing valve. In other words, in Figure 14 the range of normalized temperature ratios indicate that the ratio of cold-fluid flow to garment flow can be modulated from 0.10 to 0.90.
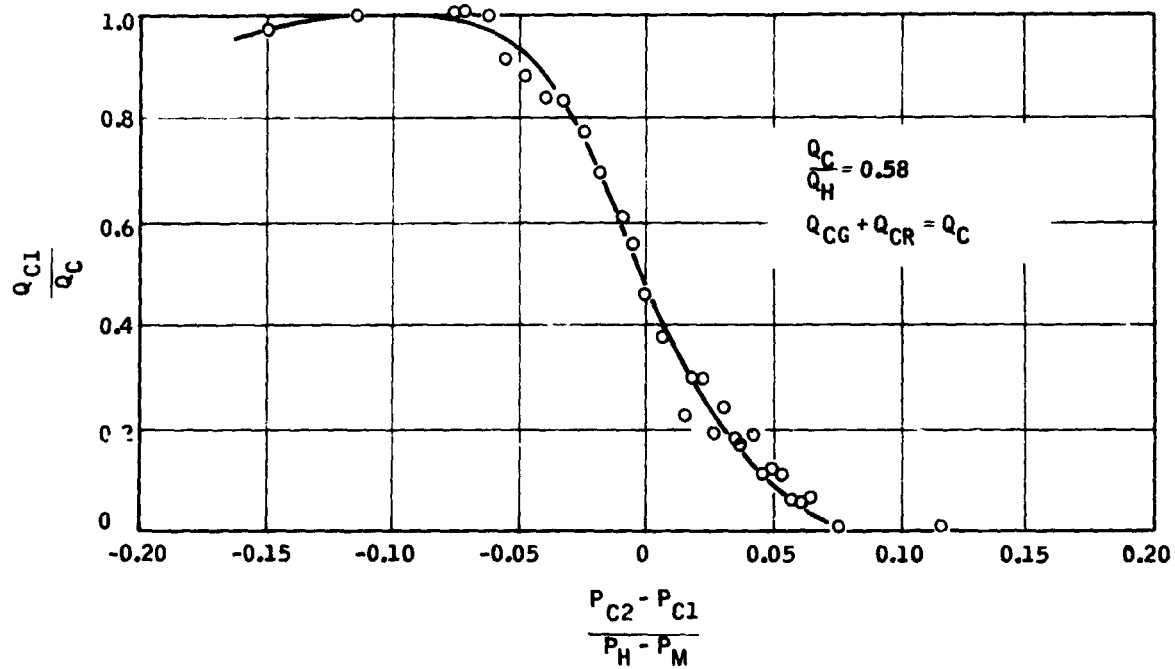
Figure 12. Mixture Ratios Produced by Model I
Fluidic Mixing Valve
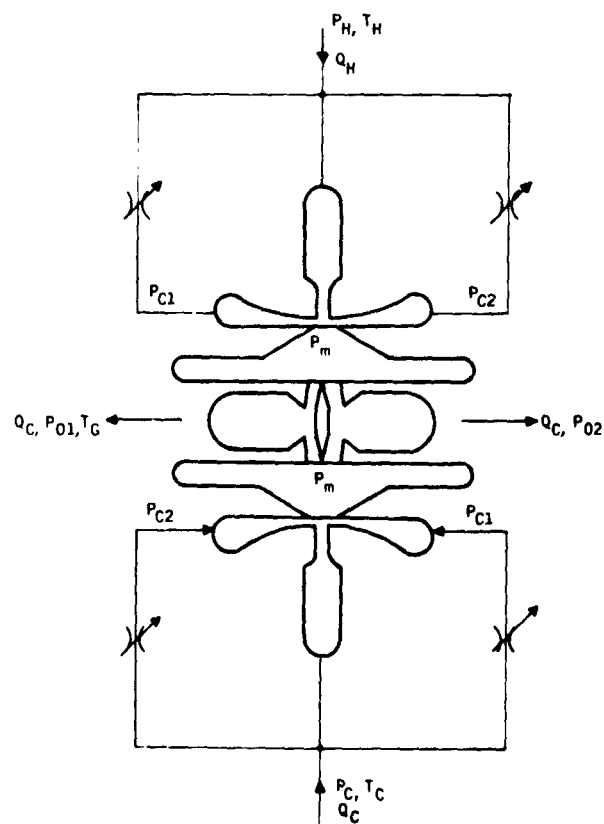
Figure 13. Fluidic Mixing Valve, Model II
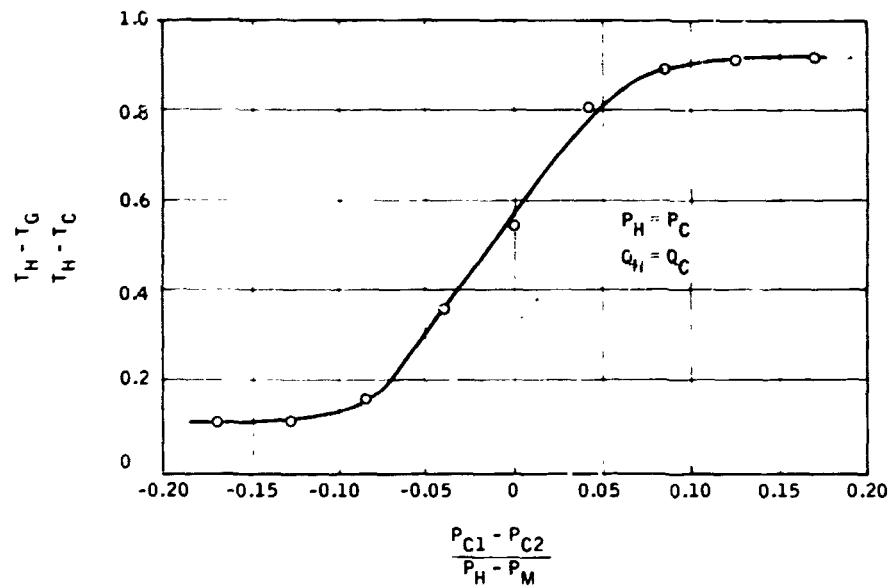
Figure 14. Mixture Ratios Produced by Model II
Fluidic Mixing Valve

The performance of Model II is superior to that of Model I in that a wider
range of mixture ratios can be achieved. According to Figure 7, the mixture
ratios from Model II can produce cooling rates from 700 to 1950 btu/hr. The
lower limit of 700 is excessive cooling for rest conditions. Through geometri-
cal changes within the device a mixture range of from zero to 1.0 should be
obtainable. However, to determine what changes should be made would require
flow visualization studies that were considered outside the scope of this pro-
gram.

Amplifier Cascades

Fluid amplifiers are required in the system to achieve adequate sensitivity
and an acceptable lower limit on cooling rate. The rate of flow into the four
control ports of the Model II fluidic mixing valve is approximately two-thirds
of the flow through the liquid-cooled garment. Consequently, to feed pressures
directly from the bridge circuit to the fluidic mixing valve would require rela-
tively large amounts of control flow out of the bridge circuit; this would result
in a relatively low sensitivity. In addition, control flow out of the bridge cir-
cuit results in residual mixing of liquid between the HEX and LCG loops; such
mixing in too great an amount results in an unacceptable lower limit on cooling
rate. These problems are circumvented through the use of jet deflection fluid
amplifiers (Figure 9) to magnify both the pressure difference signal generated
by the bridge and the flow rate of control fluid.

Pressure and flow gains can be enhanced by cascading (i.e., connecting in series) jet deflection amplifiers. Adequate sensitivity to control signals and control flow reduction by a factor of 15 were achieved by using cascades of three amplifiers each.

Pressure Level Reducer

In general, satisfactory operation of fluid amplifiers occurs only when control pressures are less than the power pressure fed to the amplifier, but greater than the pressure immediately downstream of the power jet. Referring to Figure 1, it is seen that the control pressure level generated by the bridge circuit is greater than the warm supply pressure for the fluidic controller. To operate the fluidic controller, it is therefore necessary to reduce the level of these control pressures to some value less than the warm supply pressure. In principle, this could be done by placing orifices in the control pressure lines connecting the bridge to the controller; however, such a technique would degrade pressure difference signals, thus reducing sensitivity of the system. A preferred technique is to use a fluidic momentum interchange device to reduce control pressure levels while preserving control pressure difference. Such a device is illustrated in Figure 15. Note that this fluidic device, while resembling a proportional amplifier, has no power stream. Streams fed into the inlet ports at the top of the device coalesce into a single jet. If the pressure of one stream is greater than the other, some jet deflection is produced. As in a proportional amplifier, this jet deflection results in a difference in pressure in the output legs of the device. In this way a reduction in level occurs while the pressure difference remains essentially unchanged.

Component Sizing

The selection of component sizes was based on seeking a reasonable compromise between system power consumption and controller size and weight. This selection was facilitated through a computer simulation of the circuit shown in Figure 16 and utilization of the equations listed in Appendix A.

The overall size of the controller is based primarily on the size of the power nozzle areas in the fluidic mixing valve. This is because good impedance matching between components depends on the ratio of effective flow areas in all components to the nozzle area of the fluidic mixing valve. For example, the power nozzle areas of the amplifiers immediately upstream of the mixing valve are one-half those of the mixing valve. The nozzle areas in the next amplifiers upstream are smaller again by one-half, etc. The size of the nozzle areas in the pressure level reducer are of the same order of magnitude as the effective control port areas of the first amplifiers in the cascades.

16
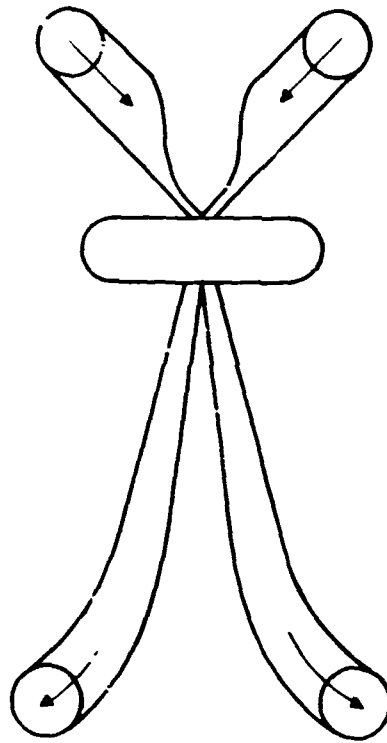
Figure 15. Control-Pressure-Level Reducer

Figure 17 presents computed ideal pump-power consumptions and controller size estimates for a range of mixing valve power nozzle areas. These data are generated for zero umbilical flow resistance. The data indicate that up to a power nozzle area of 0.010 square inch significant power reductions can be made. Beyond that point, very substantial increases in size must be made to reduce power consumption significantly, and the number of stages in the amplifier cascades must be reduced from three to two in order to keep power nozzle Reynolds numbers above 2000. In general, when power jet Reynolds numbers drop below 2000, amplifiers become noisy and unpredictable in their operation.

Based on the data in Figure 17, a mixing valve power jet cross section measuring 0.08 by 0.16 inch was selected which gives an effective area of approximately 0.0095 square inch. The mixing valve dimensions in Figure 18 and amplifier dimensions in Figure 19 are based on this area selection.

The size of the pressure level reducer shown in Figure 20 is based on the effective area required to produce acceptable control pressure levels at the first stages of the two amplifier cascades. Experiments showed that two reducers in series should be used. This combination provided the desired pressure level reduction and facilitated impedance matching that resulted in a reducer pressure difference gain of 1.0.
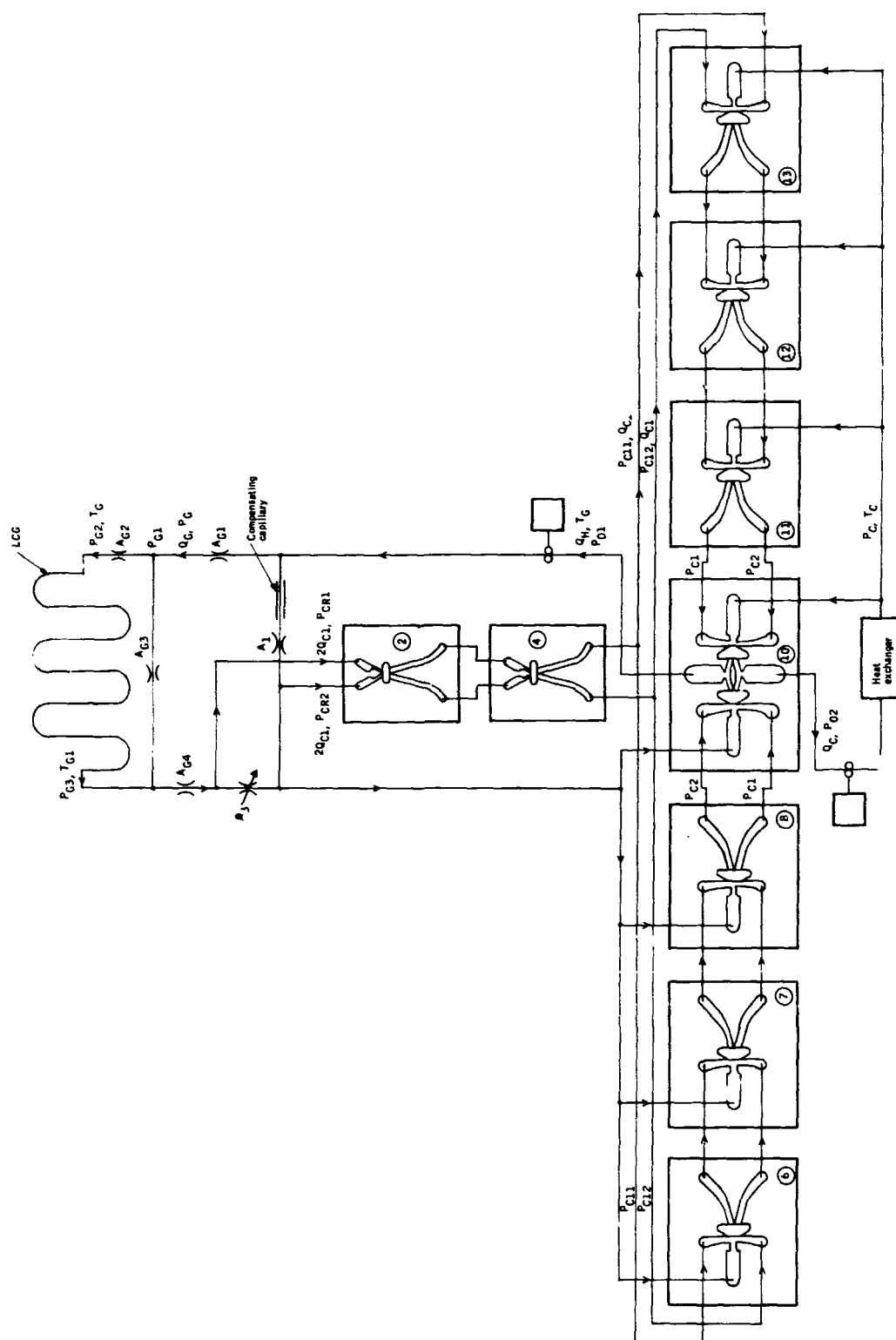
Figure 16. Control Circuit

18
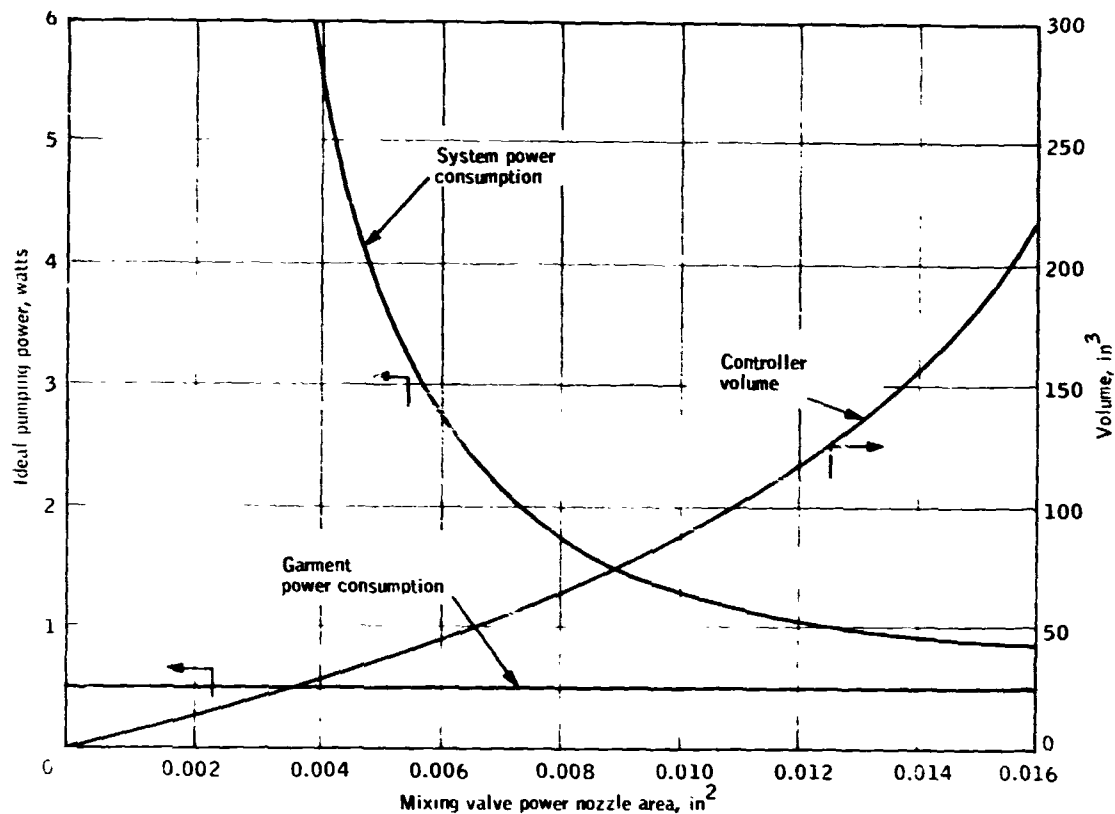
Figure 17. Variation of System Power Consumption with Size

FABRICATION AND ASSEMBLY

The components that make up the fluidic circuit were fabricated of aluminum-filled epoxy. This fabrication was accomplished by firs' machining aluminum masters, and then making silastic molds to cast components. This process was especially helpful in fabricating the amplifiers for the two cascades used in the fluidic controller. As seen in Figure 19, the various stages of the cascades differ only in the dimensions of their respective passage depths, hence one mold was used to cast all three amplifiers and the desired amplifier size was then obtained by simply machining the casting down to obtain the desired passage depths. This casting process is generally quite helpful in a developmental effort in that modifications can be made to individual castings in an attempt to improve component performance, rather than resorting to expensive alterations to the component masters.

The various fluidic components were designed such that through stacking of the components the required interconnecting passages would be automatically formed. Figures 21 and 22 illustrate the elements that form the stack which makes up the fluidic temperature controller. Figure 21 is the top view of

Figure 18. Component Dimensions -- Fluidic Mixing Valve

20

Stage	A	B	C
1	0.040	0.120	0.210
2	0.080	0.160	0.290
3	0.160	0.320	0.530

Figure 19. Component Dimensions -- Proportional
Fluid Amplifiers

Figure 20. Component Dimensions -- Signal Pressure Level Reducer

the various elements; numbers appearing beside each element indicate the order in which they are stacked from top to bottom. Stacking of these elements formed the circuit that is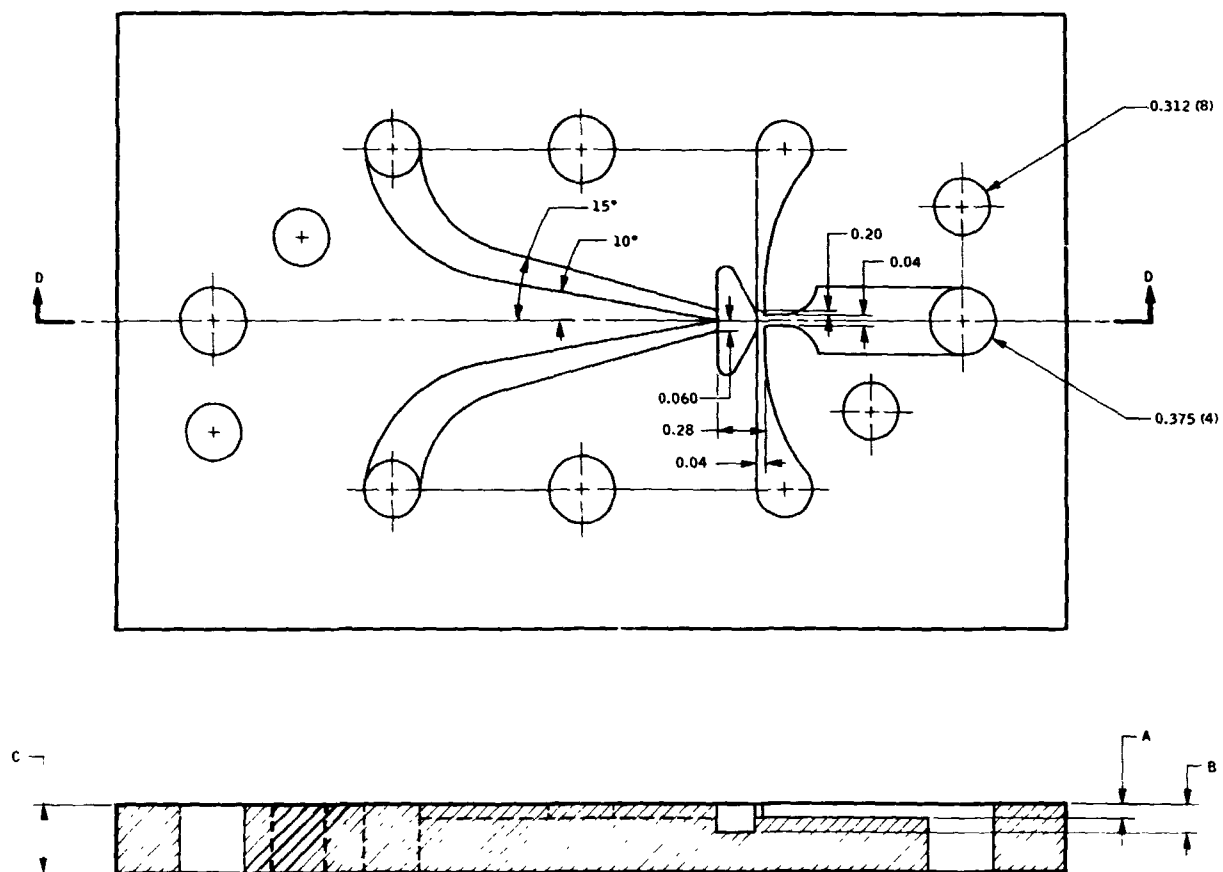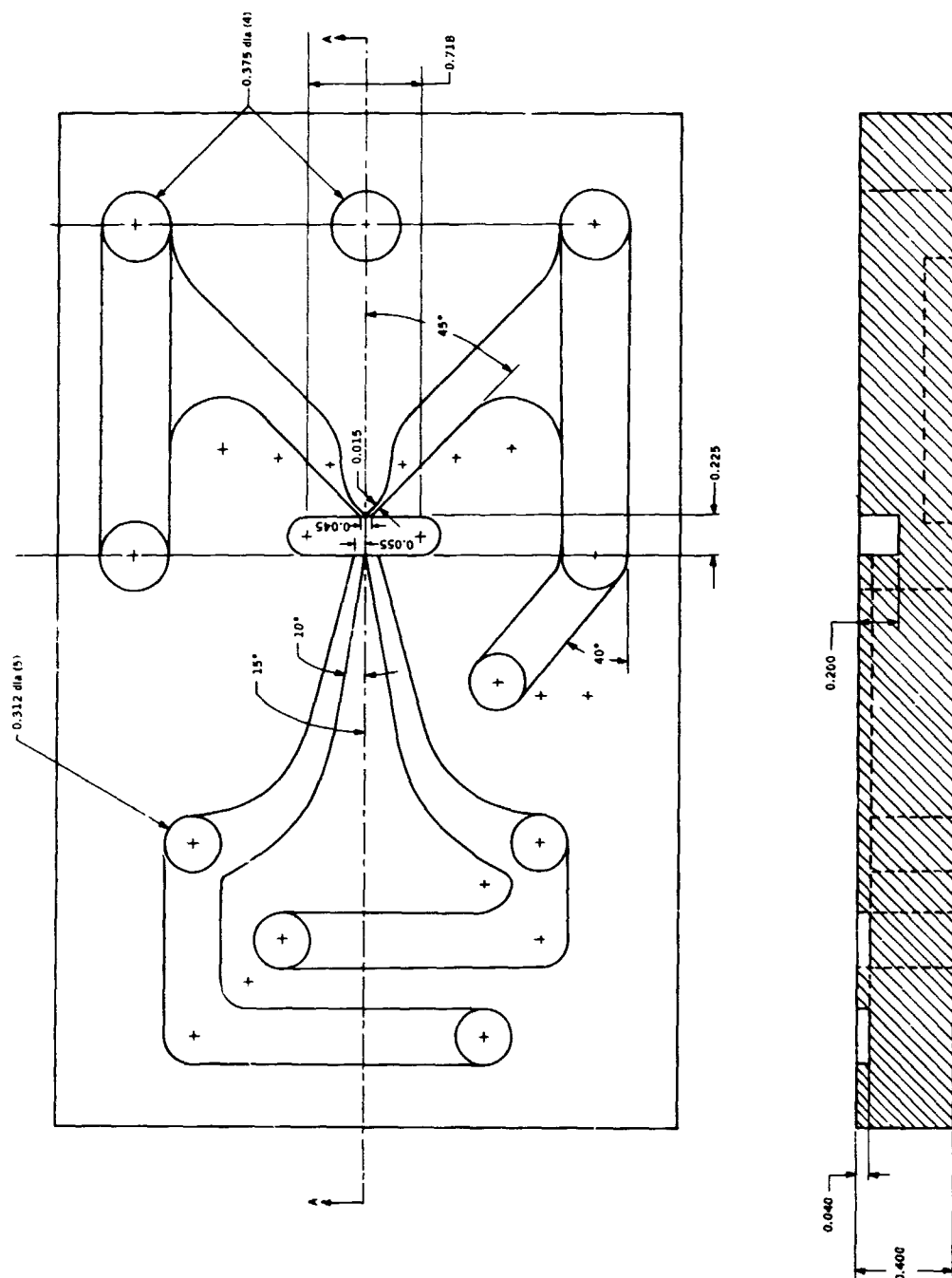 shown schematically in Figure 16. The numbers adjacent to each element correspond to the element numbers in Figures 21 and 22.

The stack of elements was assembled using a double-backed mylar tape with a synthetic rubber adhesive to form the bond between the elements. This tape is impervious to water; however, through application of naptha and use of a small wedge, the stack can be disassembled for cleaning or modification. Figures 23 and 24 show the top and bottom views, respectively, of the assembled stack. The top and bottom cover plates are brass and are provided with tube connections to interface with the remainder of the control system. In addition to the fluidic elements shown in Figures 21 and 22, it was found convenient to also locate within the fluidic controller all of the elements of the wheatstone bridge except, of course, that leg of the bridge which is made up by the garment circuit.

The hose connections to be made at the various locations are indicated in Figures 23 and 24. In Figure 24, the HEX and LCG connectors are located so as to produce an increase in cooling as the flow resistance across the garment circuit increases. If it is desired to have an increase in cooling correspond to a decrease in garment flow resistance, all that is required is that the HEX and LGC pump connections be interchanged.

Figure 25 shows the underside of the top cover plate of the fluidic controller. Built into this cover plate is the orifice, A_2, the adjustable orifice, A_3, and the capillary restriction that is provided to compensate for changes in garment flow resistance with temperature. Figure 26 illustrates a top view of the top cover plate with the small manifold cover removed. This view can be seen in the orifice, A_1, which is actually in series with a capillary restriction. Referring again to Figure 23, it is noted that the design arrangement shown provides for adjustment of orifice A_3 by means of a screw located on the face of the controller. Adjustment facilitates balancing of the fluidic control circuit for a range of umbilical lengths or garment flow resistances.

AUTOMATIC CONTROL

The function of the automatic control system for a liquid-cooled garment is to maintain a comfortable thermal state for the astronaut. This function is automatic when the control system is able to sense some index of the subject's thermal state and then modulate the temperature of the cooling water in response to changes in that index. A number of indexes can be used to measure the thermal state of a subject. For example, oxygen consumption, heart rate, and respiratory rate indicate with varied degrees of significance the rate of metabolic heat generation. Rectal, tympanic membrane, and skin temperatures indicate heat storage. A complete description of the
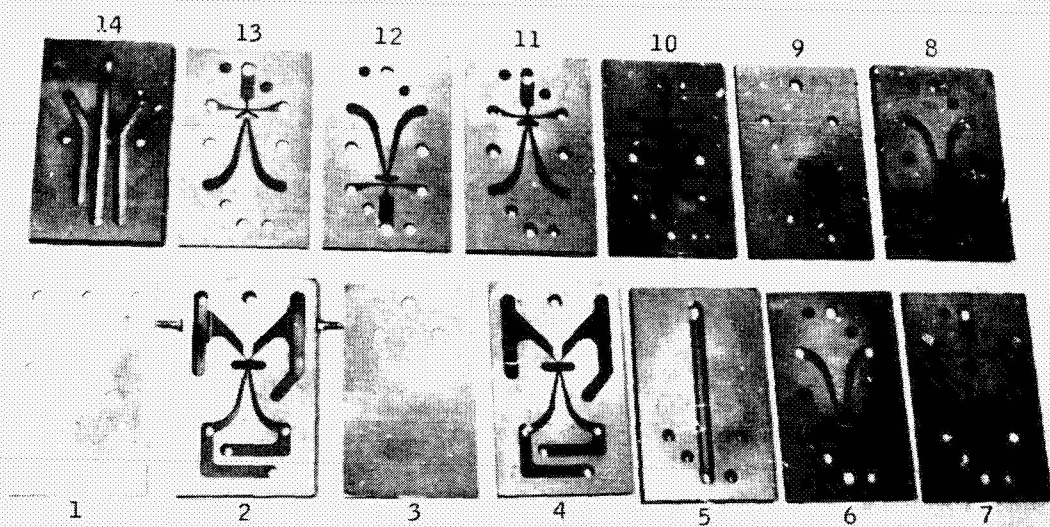
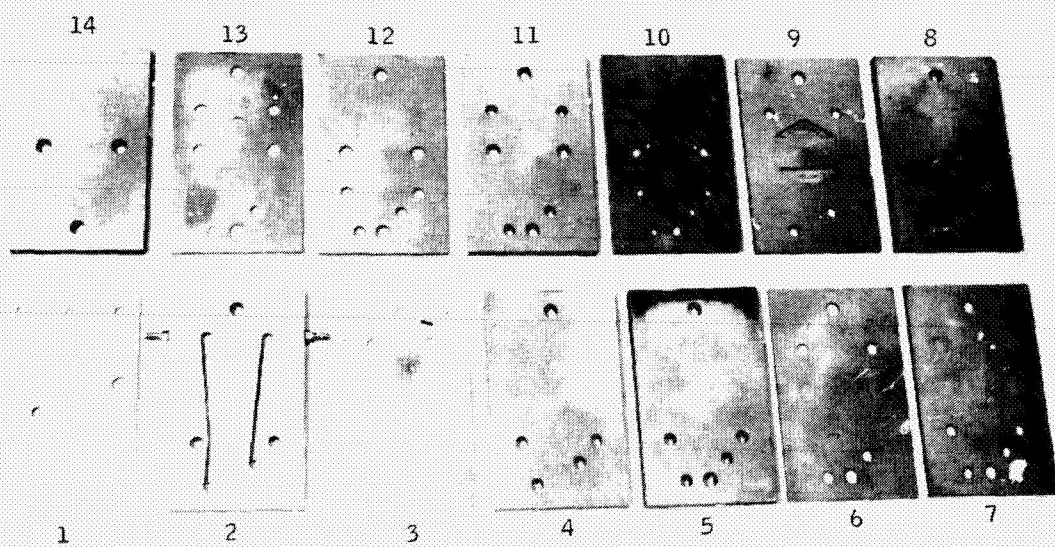Figure 21. Controller Components - Top View

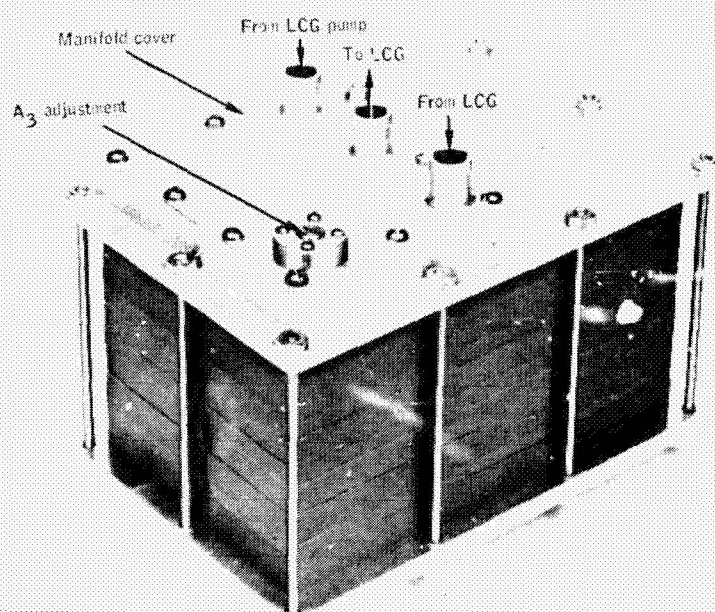Figure 22. Controller Components - Bottom View

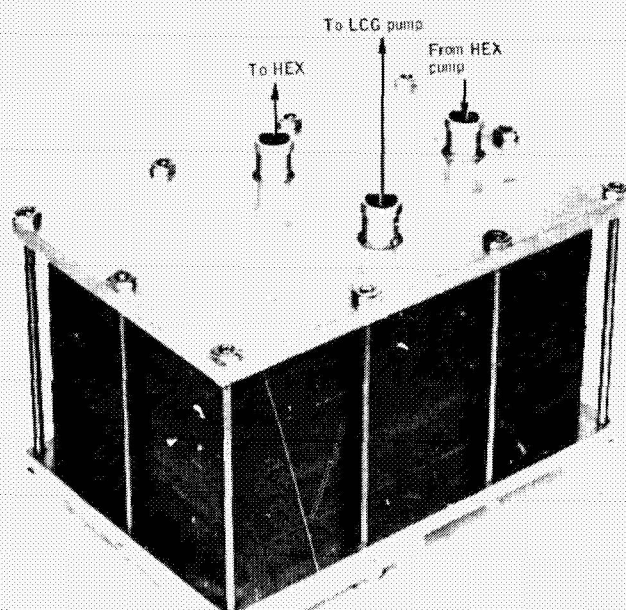Figure 23. Assembled Controller - Top View
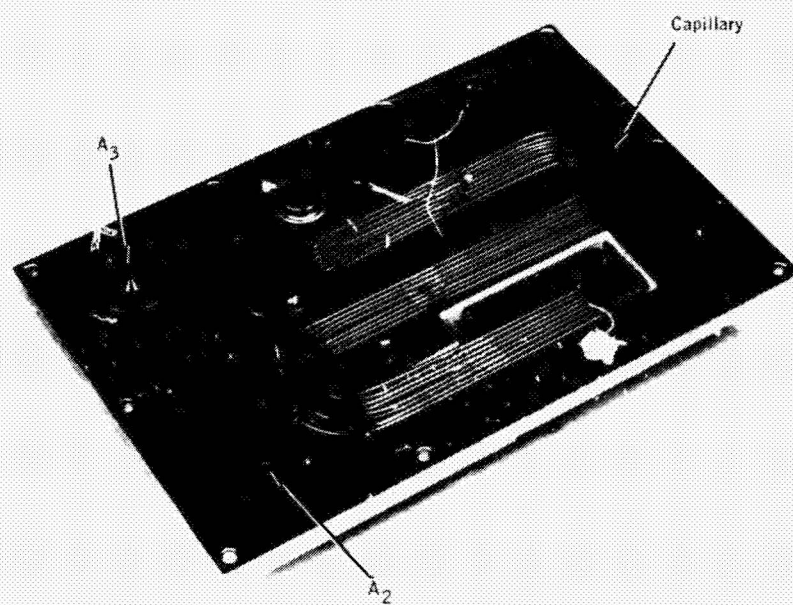

Figure 24. Assembled Controller - Bottom View

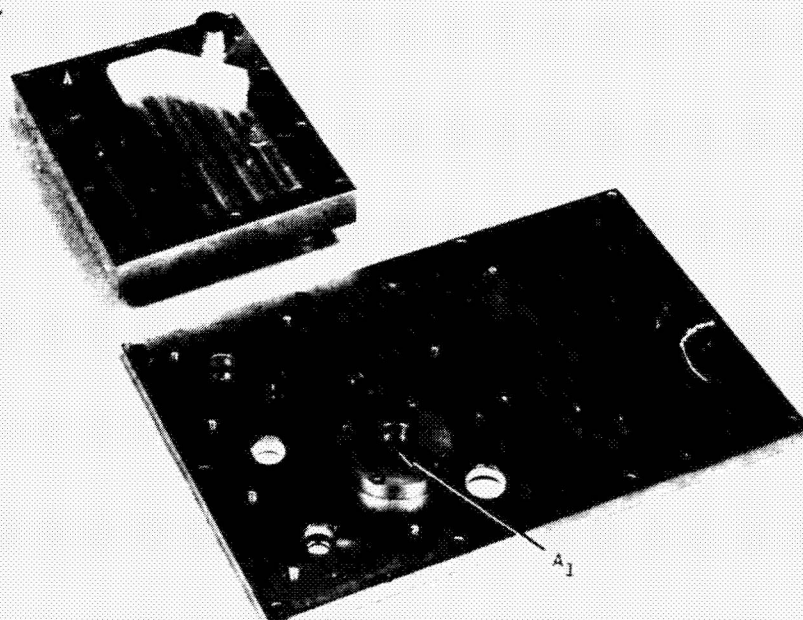Figure 25. Underside of Top Cover Plate

Figure 26. Topside of Top Cover Plate with Manifold Removed

thermal state would require measurement of several of these variables. However, from a practical point of view, only those indices accessible to the control system can be used. Skin temperature, though not entirely adequate, is therefore considered to be a very practical index of the subject's thermal state for use in automatic control systems for space suits.

Automatic temperature control was achieved in the system under discussion by using four skin temperature sensors to vary the flow resistance through the garment circuit. Skin temperature sensors used in this study are of the type developed for automatic temperature control in aircraft flight suits and are described in detail in Reference 1. Sensors used in the flight suit consisted essentially of a toluene-filled temperature bulb that actuated a small flapper valve. Toluene was considered unacceptable for space suit applications because of the fire danger that would exist in an environment of high oxygen concentration. Consequently, the sensor was modified ' utilize a noncombustible fluid for the s ising medium.

A mixture of water and glycol for use in the temperature bulb was first considered. A mixture of equal parts of water and glycol has a cubical expansion coefficient approximately one-half that of toluene. Hence, in order to obtain adequate sensitivity out of the temperature sensor, the volume of the sensing bulb was enlarged to approximately twice that used in the flight suit application. Figure 27 illustrates the temperature sensor fabricated for space suit applications.

Experiments were conducted to determine the change with skin temperature in flow area through the valve. The results shown in Figure 28 indicate a very moderate change in effective area with temperature. To increase sensitivity temperature bulbs were refilled with Freon 113 because of its higher coefficient of expansion. As indicated in Figure 28, higher sensitivity to skin temperature was obtained.

The use of the skin temperature sensors for automatic control requires that the controller possess a high gain so that the small flow area changes generated by the four skin temperature sensors will modulate cooling water temperature over a sufficient range. Analytical simulation of the control circuit on a computer indicated that the gain of the controller could be easily changed by simply varying the size of the orifice, A_1, which is in series with the temperature-compensating capillaries. Data generated through computer studies indicated that the gain could be increased to the point where the system actually became bistable. As an example, Figure 29 shows computer-generated curves for two values of orifice area, A_1. With an area of 0.000818 square inch a reasonably high system gain is obtained. For a somewhat larger value of A_1, the curve becomes "S" shaped, and under this condition would actually be bistable. Based on this computer data and the experimental results in Figure 28, it was concluded that four skin temperature sensors could produce a maximum change in coolant temperature if the sensor temperature were to change by only 4°F. This sensitivity appeared to be adequate in that skin temperatures above active muscles during exercise can change as much as 8°F.
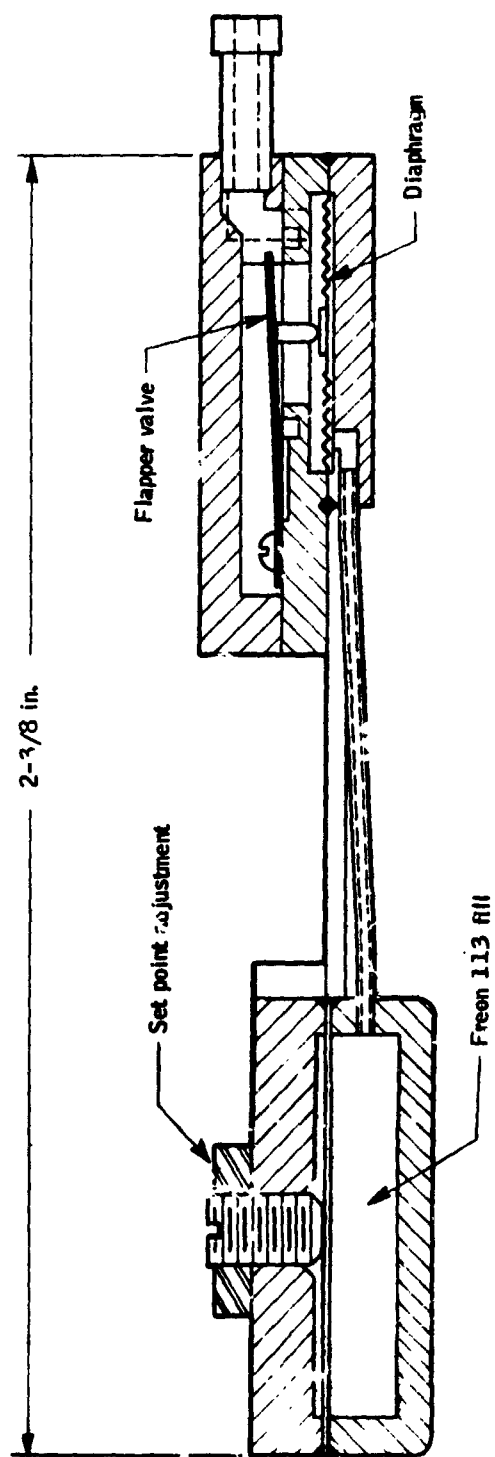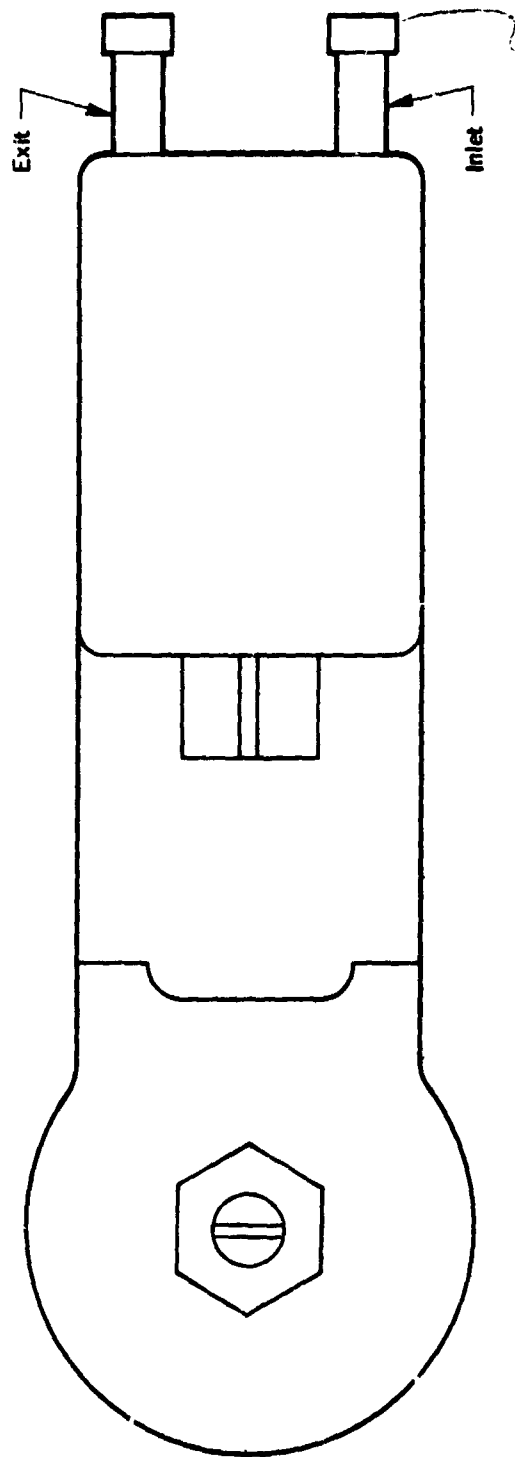
Figure 27. Skin-Temperature Sensor

Exit

Inlet

Flapper valve

Set point adjustment

2-3/8 in.

Diaphragm

Freon 113 fill
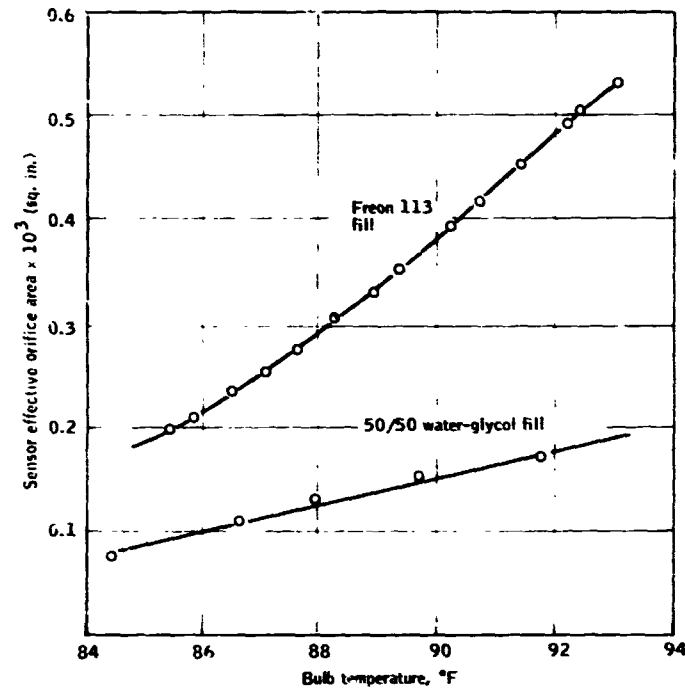
Figure 28. Variation of Sensor Effective Orifice
Area with Temperature
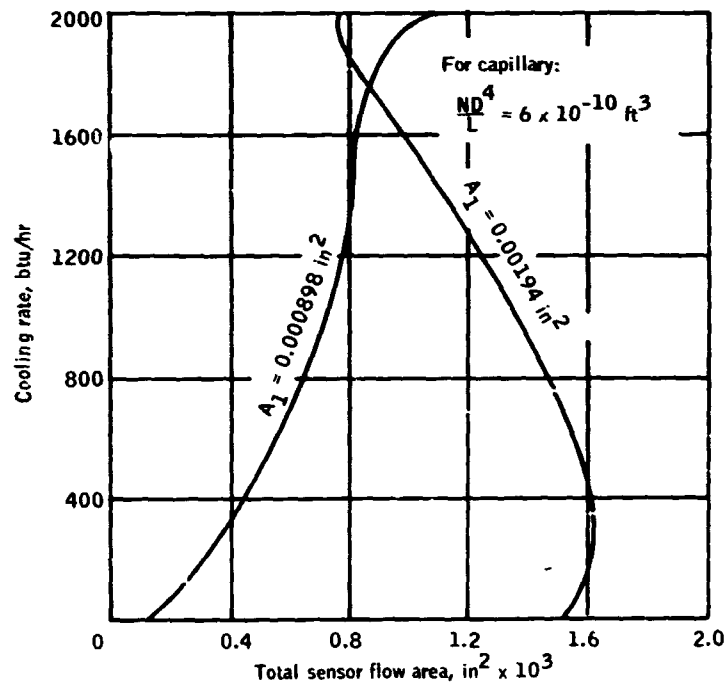
Figure 29. Controller Gain Variation with Area A_1

Two of the sensors were installed on the legs above the calf muscles in order to achieve temperature response to leg exercise, and two sensors above the pectoral muscles on the upper torso in order to achieve response to arm exercise. Preliminary tests of the circuit revealed that whereas adequate gain could be achieved to modulate the coolant temperature over the maximum range, signal noise associated with thermal transients and small temperature fluctuations made the system unstable. Consequently, the system gain was reduced by further decreasing the size of the orifice, A_1. In

order to obtain sufficient sensitivity to skin temperature, it was then necessary to place 0.032-inch orifices in series with the cooling passages of the liquid-cooled garment as shown in Figure 30. This modification had the undesirable effect of increasing the pressure drop across the liquid-cooled garment, thus increasing the power consumption of the overall circuit. However, for purposes of demonstration of the automatic control concept, this course of action was justified.

0.032-inch
dia. orifice

Skin temperature sensor
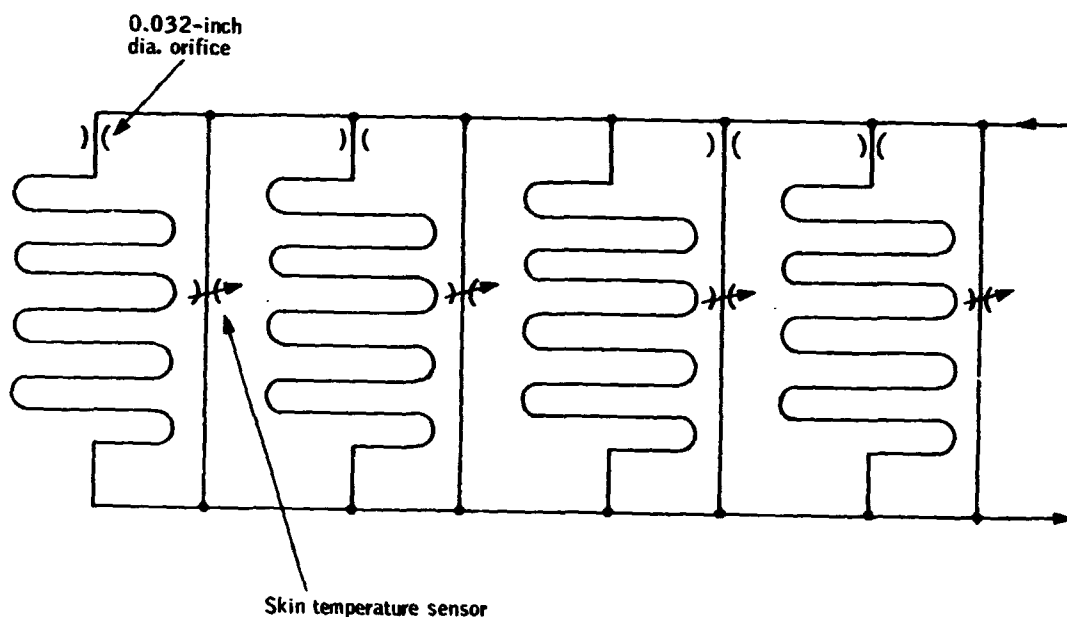
Figure 30. Garment Circuit Using Series Orifices for
Increasing Sensor Effectiveness

Experiments were conducted to examine the operation of the control circuit in an automatic mode. Extreme difficulty was encountered in balancing the system so that when the subject was at rest, control pressure differentials fell within the band corresponding to that which produces variations in coolant temperature. On a few occasions this condition was nearly achieved, and data typical of that shown in Figure 31 was obtained during exercise. Note that the temperature of the sensors above the calf muscles increased by approximately 8 °F during exercise. However, because the control pressure differential generated by the system when the subject was at rest did not fall within the band which modulates coolant temperatures, the leg temperature had to rise approximately 4°F before coolant temperature was automatically reduced. Generally, reduction of coolant temperature illustrated was inadequate to keep the subject comfortable.

Although these data do not indicate that the system as tested gives adequate comfort control in an automatic mode, they demonstrate that the basic principle of using skin temperature to automatically reduce coolant temperature is feasible. It is highly probable that through further development of skin temperature sensors to achieve larger changes in effective flow area with skin temperature, and the devising of adequate balancing techniques to ensure that the system is operating within the correct band of control pressure differentials, that an effective automatic system could be developed. Location of sensors to achieve optimum control is also an area in need of additional investigation.

MANUAL CONTROL

Because of the difficulties encountered in developing the automatic aspects of this system, efforts were directed late in the study toward developing an effective manual control system. Because the fluidic valve could not generate flow mixture ratios under 0. 10, maximum temperature that could be achieved in the LCG loop was approximately 60°F (although through further mixing valve development its performance could be improved so that higher temperatures in the LCG loop could be obtained). It was decided that the manual control valve should be developed so as to provide for a sufficiently low cooling rate so that subjects would not be uncomfortable at rest conditions. This was accomplished by flow rate modulation.

A manual control circuit designed to modulate both flow rate and temperature is shown schematically in Figure 22. This circuit embodies two three-way valves, one fixed orifice, and two variable orifices. In principle, the function of this circuit could be embodied in a single specially-designed manual control valve for the liquid-cooled garment. The circuit is designed so that when three-way valves 1 and 2 are bypassing flow, the restriction A_0 is such that only approximately 40 lbs per hour of liquid circulates through the liquid-cooled garment. Also, orifices A_{BP2}, A_{BP1} are set so that the control pressure differential generated in the bridge circuit calls for the maximum garment inlet temperature (in this case 60°F). The relative values of the
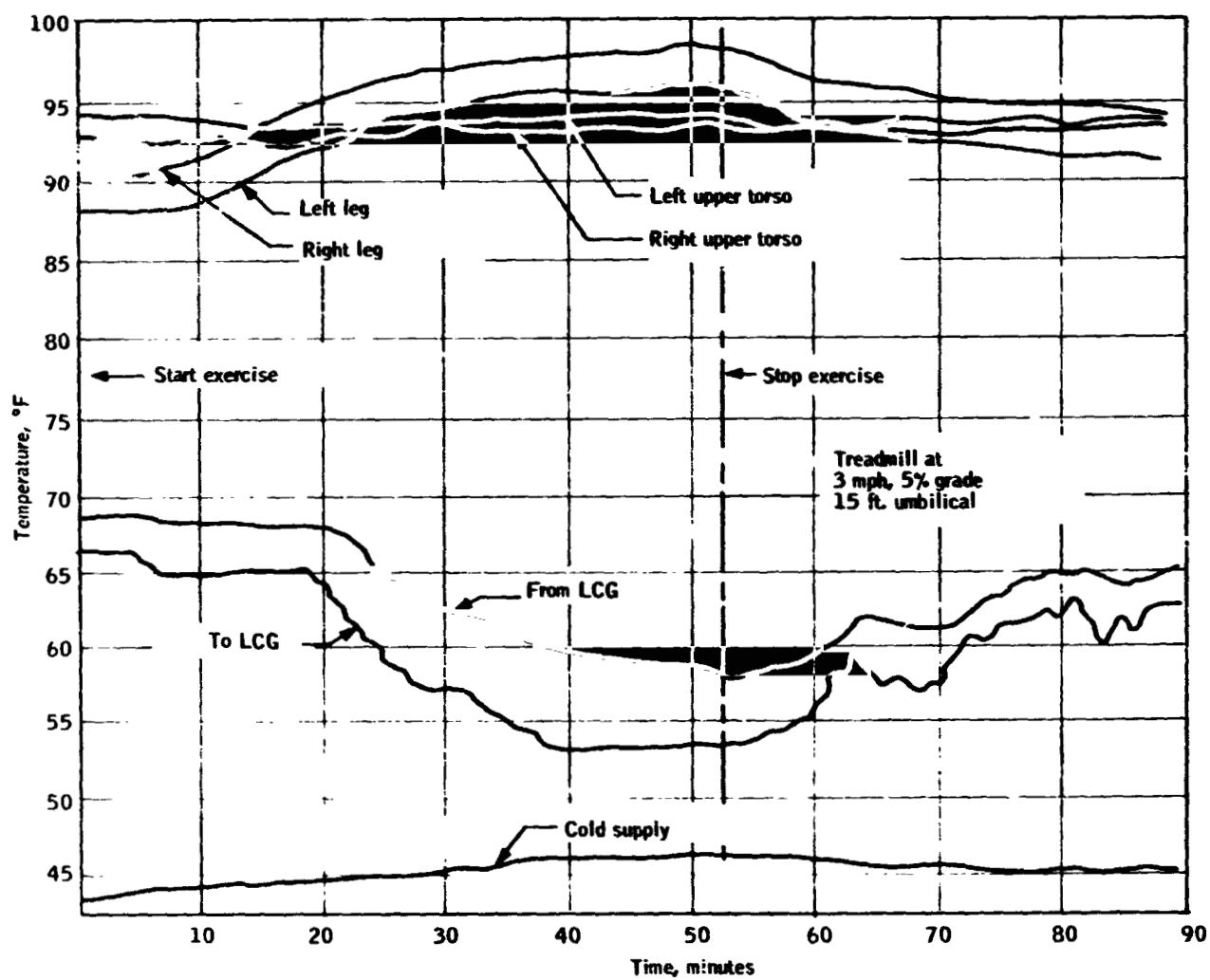
Figure 31. Automatic Response of System to Treadmill Exercise

0.045 in.
orifice (A_0)

3-way
no. 1

3-way
no. 2
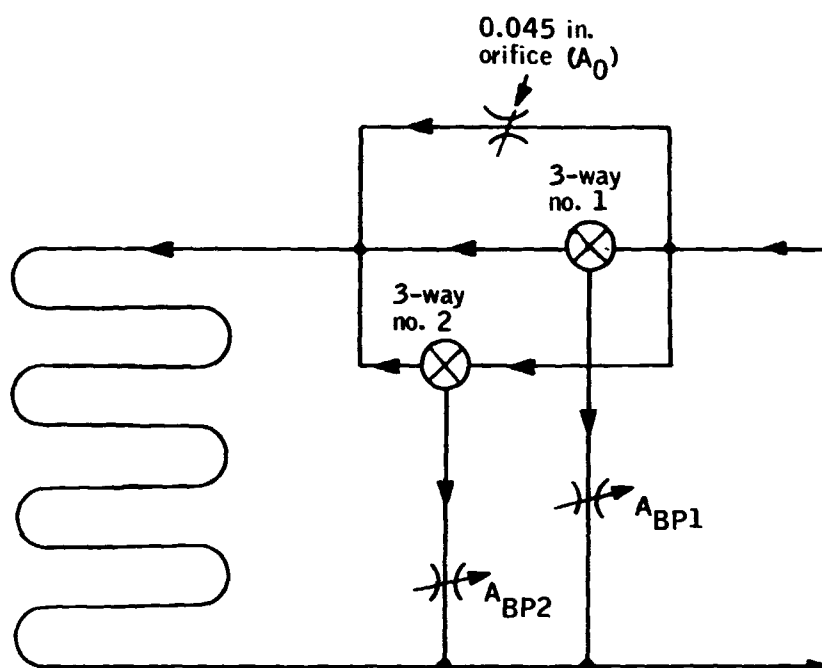
A_{BP1}

A_{BP2}

Figure 32. Garment Circuit for Manual Control

areas A_{BP2} and A_{BP1} are such that when three-way valve 1 is switched to circulate more water through the water-cooled garment, then concurrently the control pressure differential generated in the fluidic controller is zero, and an inlet temperature of approximately 50°F is generated. Switching three-way valve 2 further reduces the inlet temperature to approximately 45°F.

Experiments were also conducted to determine the dynamic response of the system to a manual input control signal. Figure 33 illustrates data acquired for two umbilical lengths. The responses generated using either of the umbilical lengths have certain similar characteristics. For example, the temperature change at the controller exit is almost immediate, whereas there is a finite delay before the temperature at the inlet of the liquid-cooled garment begins to drop. This delay is related to the time required for fluid to travel the umbilical length. Note that the time delay for the 15-foot umbilical is significantly less than that for the 60-foot umbilical. Both umbilical lengths exhibit a rather slow increase in garment inlet temperature after a warming signal is generated. The rate at which this temperature increases during warming is limited by the rate at which the body can generate heat. A 60-foot umbilical with tubes of 3/8 in. inside diameter contains approximately 5 lbs water. When a subject is at rest and generating approximately 400 BTU's per hour, the maximum rate at which the temperature in the LCG loop could increase is approximately 70°F per hour. The relation

33
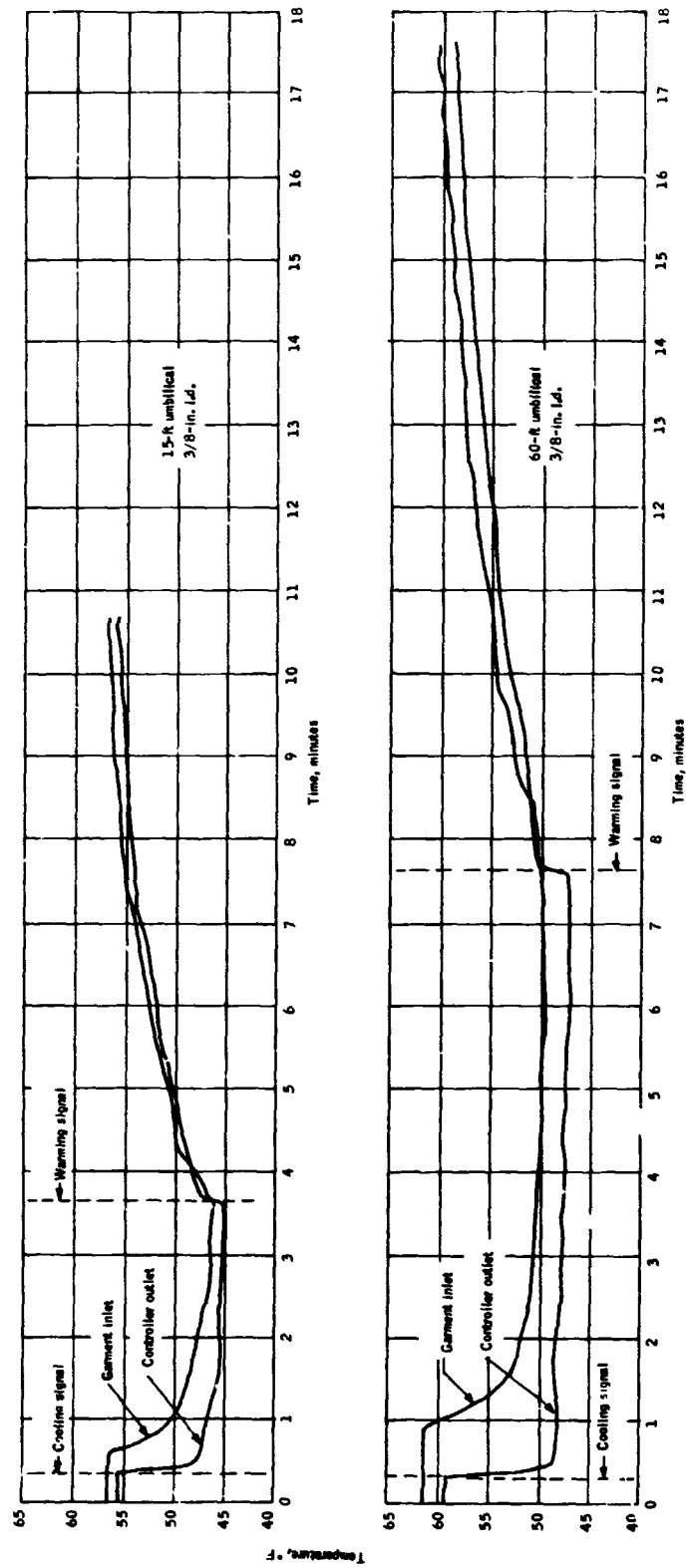
Figure 33. Dynamic Response of Manual Control System

between the warming rate and the amount of water circulating through the umbilical is apparent from the data in that the warming rate with a 15-foot umbilical is significantly greater than with a 60 foot umbilical.

CONCLUSIONS

1. Garment inlet temperatures can be modulated during EVA by using already-existing supply and return lines for transmission of pressure signals.

2. Fluidic techniques that require no moving parts can be used to perform coolant temperature modulation through the mixing of warm and cold streams.

3. A given fluidic controller can be readily adjusted to operate with varying umbilical lengths of up to 60 feet.

4. Automatic system operation based on the use of skin-temperature. sensors appears feasible. Successful implementation will require sensors that produce large flow resistance changes with skin temperature, and further study to determine optimum sensor location.

5. Manual operation over a sufficiently-wide range of cooling rates is achieved through combined flow and temperature modulation. Additional controller development should facilitate cooling rate modulation through temperature variation alone.

APPENDIX A

SYSTEM ANALYSIS

An analytical description of the fluidic control circuit was developed to facilitate design optimization and provide understanding of the circuit operation. This description, when programmed on an automatic digital computer, facilitates rapid determination of the effects of changing various parameters on overall circuit characteristics.

A schematic of the circuit under consideration is illustrated in Figure 16. Pressure, temperature and volume-flow-rate nomenclature are as indicated.

Component Description

The control circuit utilizes three basic fluidic elements: 1) a fluidic mixing valve; 2) cascaded proportional amplifiers; and 3) a control-pressure-level reducer. An analytical description of each follows.

Fluidic mixing valve. - The physical features of the fluidic mixing valve were described in the main body of this report. Analytically, the valve can be treated as an equivalent circuit of valves as indicated in Figure A1. The circuit is operated so that

$$A_A + A_B = A_C + A_D = A_M \tag{A1}$$

where A_M is a constant. Under these conditions, flows into and out of the mixing valve can be described by orifice flow equations:

$$Q_H = A_M \sqrt{\frac{2}{\rho} (P_H - P_{01})} \tag{A2}$$

$$Q_C = A_M \sqrt{\frac{2}{\rho} (P_H - P_{02})} \tag{A3}$$

In the actual circuit $Q_H = Q_C$, so that symmetry requires that $P_{01} = P_{02}$. The area A_M is related to the power port area A_{PM} of the fluidic mixing valve by the equation

$$A_M = C_D A_{PM} \tag{A4}$$

The value of C_D, experimentally determined, is approximately 0.975.
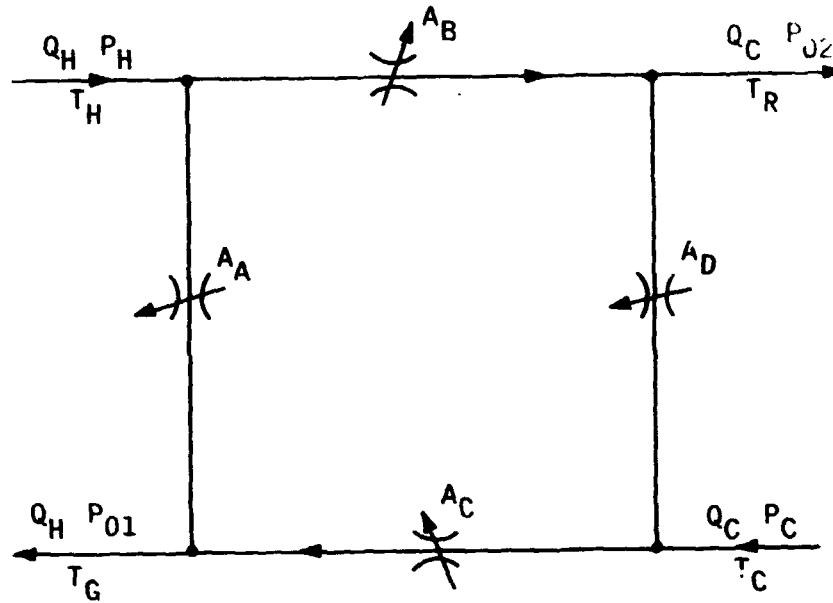
Figure A1. Fluidic Mixing Valve;
Equivalent Circuit

Temperature modulation is achieved by the mixing valve through, in effect, modulating the areas of orifices A, B, C and D under the restriction expressed in Equation (A1). The temperature T_G of one fluid stream leaving the valve is reduced by opening orifices B and C and closing orifices A and D. The maximum T_G will occur when orifices C and B have minimum flow area while orifices A and D have maximum flow area.

The effective variations of orifice flow areas have been determined experimentally. Temperatures of streams entering and leaving the fluidic mixing valve have been measured and flow rates within the valve deduced from a simple heat balance. The experimental data are shown in Figure 14. The control pressure difference $(P_{C1} - P_{C2})$ required to produce a given mixture ratio is normalized by the dynamic pressure of the power jets within the fluidic mixing valve. Experimentally, the dynamic pressure has been found to be

$$P_{DM} = 0.87 \, (P_H - P_{01})$$
$$= 0.87 \, (P_C - P_{02}) \tag{A5}$$

The mixing valve characteristic indicated by Figure 14 can be approximated analytically by the equation

$$\lambda = 0.45 \left\{ 1 - \sin \left[17.5 \left(\frac{\left| P_{C1} - P_{C2} \right|}{P_{DM}} \right) \right] \right\} \tag{A6}$$

where

$$\lambda = \frac{T_H - T_G}{T_H - T_C}$$

Cascaded proportional amplifiers. - Cascades of proportional amplifiers are used to reduce the amount of control flow required to drive the fluidic mixing valve and increase its sensitivity to pressure signals generated by the bridge circuit. The cascade is designed so that the effective power port area of each amplifier is twice that of the amplifier that is immediately upstream. This size ratio results in reasonable compromise between pressure gain and flow-rate gain per stage.

If each amplifier of a cascade of N_S elements has a pressure gain G_p, then the pressure-difference signal generated in the mixing-valve control ports is related to the pressure-difference signal at the first amplifier in the cascade by the expression

$$\frac{P_{C1} - P_{C2}}{P_{C11} - P_{C12}} = G_p^{N_S} \tag{A7}$$

The dynamic pressure of the power jet in each amplifier increases by a factor G_D per stage moving downstream. Hence, the power-jet dynamic pressure in the first amplifier of the cascade is

$$P_{D1} = P_{DM} G_D^{-N_S} \tag{A8}$$

The cascade used in this study exhibits a G_D of 1.5.

Fluid entering the control ports of the first amplifier of the cascade can be viewed as flow through an orifice-type restriction. The effective orifice area of the control ports is a function of the amplifier geometry and can be expressed as

$$A_{C1} = R_C A_{P1} \tag{A9}$$

where A_{P1} is the effective power port area of the first stage of the amplifier cascade. For the amplifiers used in this study, R_C is approximately 0.5. A_{P1} is related to the power port area of the mixing valve by the expression

$$A_{P1} = 2^{-N_S} A_{PM} \tag{A10}$$

so that

$$A_{C1} = 2^{-N_S} R_C A_{PM} \tag{A11}$$

The pressure downstream of the first-stage control ports is taken as $(P_C - P_{D1})$ or $(P_H - P_{D1})$, and the upstream pressure as P_{C11} or P_{C12}. In reality, difference between P_{C11} and P_{C12} remains relatively small, so that the control flow can be based on the average control pressure

$$\bar{P}_{C1} = \frac{1}{2}(P_{C11} + P_{C12}) \tag{A12}$$

The flow into a control port of the first stage of the amplifier cascade is thus

$$Q_{C1} = 2^{-N_S} R_C A_{PM} \sqrt{\frac{2}{\rho}\left[\bar{P}_{C1} - (P_C - P_{D1})\right]} \tag{A13}$$

Control-pressure-level reducer. - Effective operation of a proportional amplifier requires that the average control pressure level be below the total pressure of the amplifier power jet. The level of control pressures generated by the bridge circuit shown in Figure 16 is in general higher than either P_H or P_C.

Orifices could be used to reduce pressure levels before the fluid enters the control ports of the amplifier, but this would degrade the difference signal generated by the bridge circuit. A preferred technique is to use a pressure level reducer described in the main body of this report. This device reduces the control pressure level while maintaining the control pressure difference, i.e.

$$(P_{CR1} - P_{CR2}) \approx (P_{C11} - P_{C12}) \tag{A14}$$

Sizing of the reducer depends on the rate of control flow, the increment of pressure reduction required, and the effective orifice area of the control ports of the first stage of the amplifier cascade. The reducer can be viewed, for sizing purposes only, as one orifice in series with a circuit of four orifices in parallel, each representing an amplifier control port of effective area A_{C1}. The pressure entering the reducer is taken as the average

$$\bar{P}_{CR} = \frac{1}{2}(P_{CR1} + P_{CR2}) \tag{A15}$$

40

so that

$$A_R = \frac{4Q_{C1}}{\sqrt{\frac{2}{\rho}} \, (\bar{P}_{CR} - \bar{P}_{C1})} \tag{A16}$$

Bridge Circuit

The bridge circuit is designed to generate a pressure difference signal in response to changes in flow resistance across the "garment circuit". The "garment circuit" is made up of the liquid-cooled garment, umbilical, manual control valve, and skin-temperature sensors.

Referring to Figure 16, based on continuity, the flow through A_2 is

$$(Q_H - Q_G - 2Q_{C1}) = A_2 \sqrt{\frac{2}{\rho}} \, (P_{CR2} - P_H) \tag{A17}$$

Similarly, the flow through A_3 is

$$(Q_G - 2Q_{C1}) = A_3 \sqrt{\frac{2}{\rho}} \, (P_{CR1} - P_H) \tag{A18}$$

Consequently, the control pressure difference generated by the bridge is

$$P_{CR1} - P_{CR2} = \frac{\rho}{2} \left[\left(\frac{Q_G - 2Q_{C1}}{A_3} \right)^2 - \left(\frac{Q_H - Q_G - 2Q_{C1}}{A_2} \right)^2 \right] \tag{A19}$$

Equation (A19) can be used to compute the required flow rate through the garment circuit Q_G. This is accomplished by first stipulating what value of $(P_{C1} - P_{C2})/P_{DM}$ needed for the fluidic mixing valve [as seen in Figure 14, this stipulates a certain value of $(T_H - T_G)/(T_H - T_C)$]. The mixing valve dynamic pressure P_{DM} is computed from Equation (A5), and the control pressure difference $(P_{C11} - P_{C12})$ is computed from Equation (A7). The pressure difference required of the bridge circuit is then

$$P_{CR1} - P_{CR2} = \frac{P_{C11} - P_{C12}}{G_R} \tag{A20}$$

41

where G_R is the pressure gain of the pressure level reducer. G_R is 1.0 for reduce: . d in this study. With $(P_{CR1} - P_{CR2})$ determined from Equation (A. , $\cdot_{C1}$ from Equation '.13), and Q_H stipulated, Q_G can be determined from Equation (A19). The ind'vidual pressures P_{CR2} and P_{CR1} can then be computed using Equations (A17) and (A18), respectively.

The pressure P_G is computed by adding the pressure drops through the capillary and the orifice A_1 to P_{CR2}. The equation that accomplishes this is

$$P_G = P_{CR2} + \frac{\rho}{2}\left(\frac{Q_H - Q_G}{A_1}\right)^2 + \frac{128\mu}{\pi C}(Q_H - Q_G) \tag{A21}$$

where

$$C = \frac{N_T D_T}{L_T}$$

The parameter C characterizes the capillary geometry.

The bridge circuit analysis is completed by sizing the garment circuit components to produce a pressure drop $(P_G - P_{CR1})$ with a flow rate Q_G. As noted in Figure '3, the garment circuit includes the garment itself plus orifices in series ' parallel. These orifices may represent manually operated valves, skin te_ ,.:rature sensors, and umbilical flow resistances. The usual computational procedure is to assign fixed values to A_{G1} and A_{G4}, and compute a range of combinations of A_{G2} and A_{G3} that will satisfy the pressure drop and flow rate required of garment circuit.

The pressure P_{G1} and P_{G3} are computed simply from the uations

$$P_{G1} = P_G - \frac{1}{2}\rho\left(\frac{Q_G}{A_{G1}}\right)^2 \tag{A22}$$

$$P_{G3} = P_{CR1} + \frac{1}{2}\rho\left(\frac{Q_G}{A_{G4}}\right)^2 \tag{A23}$$

Note that indiscrete selections of A_{G1} and A_{G4} can lead to the fallacious case v here P_{G3} is greater than P_{G1}.

The remainder of the garment circuit solution requires iteration because the garment fl· ·· resistance is sensitive to inlet pressure and temperature. In general, ge r ment flow '.. represented by the expression

$$P_{G2} - P_{G3} = \alpha\, Q_{G1} + \beta\, Q_{G1}^{\,2} \qquad\qquad (A24)$$

α and β are functions of garment inlet pressure and temperature. By curve fitting Equation (A24) to experimental data, the numerical values of α and β shown in Table A1 have been determined. Since α and β are functions of P_{G2}, it is convenient to rearrange Equation (A24) to obtain an explicit expression for Q_{G1} rather than P_{G2}. The correct root of Equation (A24) is

$$Q_{G1} = \frac{1}{2\beta}\left[-\alpha + \sqrt{\alpha^2 + 4\beta\,(P_{G1} - P_{G3})}\,\right] \qquad\qquad (A25)$$

The flow through A_{G2} is

$$Q_{G1} = A_{G2}\sqrt{\frac{2}{\rho}\,(P_{G1} - P_{G2})} \qquad\qquad (A26)$$

and through A_{G3} is

$$Q_G - Q_{G1} = A_{G3}\sqrt{\frac{2}{\rho}\,(P_{G1} - P_{G3})} \qquad\qquad (A27)$$

Equations (A24), (A25), and (A26) form a set of three independent equations which may be solved iteratively for Q_{G1}, P_{G3} and either A_{G2} or A_{G3}. A tested procedure is to compute A_{G3} for a range of assumed values of A_{G2}.

TABLE A1

CONSTANTS FOR COMPUTING

$$P_{G2} - P_{G3} = \alpha\rho Q_{G1} + \beta(\rho Q_{G1})^2.$$

$$\rho Q_{G1} \sim \text{LB.\,/HR}$$

$T_G(°F)$	$P_{G2}(PSIG)$	$\alpha \times 10^2$	$\beta \times 10^5$
42	8.8	0.856	0.205
		0.768	0.166
		0.660	0.140
61	14.7	0.790	0.182
		0.684	0.152
		0.518	0.146
80	20.6	0.722	0.165
		0.618	0.137
		0.480	0.125

Cooling Rates and Temperatures

The circuit temperature and cooling rate estimates can be based on basic heat transfer and energy conservation considerations. The liquid-cooled garment is treated as heat transfer from a surface at uniform temperature $\overline{T}_s$ to a flowing fluid. Based on equations in reference 2, the temperature rise across the liquid-cooled garment is

$$\frac{T_{G1} - T_G}{\overline{T}_s - T_G} = 1 - e^{-\xi} \tag{A28}$$

where

$$\xi = \frac{UA_s}{\rho c Q_{G1}} \tag{A29}$$

Energy balances lead to the expressions

$$T_G = \lambda T_C + (1-\lambda) T_H \tag{A30}$$

$$T_{G1} = \gamma T_H - (\gamma-1) T_G \tag{A31}$$

where

$$\gamma = \frac{Q_H}{Q_{G1}} \tag{A32}$$

By combining Equations (A28), (A30) and (A31), T_{G1} and T_G can be eliminated, and there results

$$T_H = \frac{\overline{T}_s(1-e^{-\xi}) + \lambda \left[(\gamma-1) + e^{-\xi}\right] T_c}{(1-e^{-\xi}) + \lambda \left[(\gamma-1) + e^{-\xi}\right]} \tag{A33}$$

The temperatures T_{G1} and T_G can now be computed from Equations (A30) and (A31), respectively.

The rate of heat transfer to the liquid-cooled garment is

$$q = \rho c \, Q_{G1} (T_{G1} - T_G) \tag{A34}$$

By combining this expression with Equation (A28), one obtains

$$q = \rho c \, Q_{G1} (\overline{T}_s - T_G) (1 - e^{-\xi}) \tag{A35}$$

44

The temperature and heat transfer equation and bridge pressure equations are interrelated by virtue of the temperature dependence of the viscosity term appearing in Equation (A21). Precise solutions will therefore require an iterative loop at this point in an automatic computer program.

APPENDIX B
NOMENCLATURE

A_A, A_B, A_C, A_D equivalent circuit orifice areas, ft^2 (see fig. A1)

A_{G1}, A_{G2}, A_{G3}, A_{G4} garment circuit orifice areas, ft^2 (see fig. 16)

A_1, A_2, A_3 bridge circuit orifice areas, ft^2 (see fig. 16)

A_0, A_{BP1}, A_{BP2} manual control circuit orifice areas, ft^2 (see fig. 32)

A_{C1} amplifier control port effective area, ft^2

A_M mixing valve effective flow area, ft^2

A_{PM} mixing valve power port area, ft^2

A_{P1} amplifier power port area, ft^2

A_R pressure reducer effective orifice area, ft^2

A_S skin surface area subjected to cooling, ft^2

c specific heat of water, Btu/slug °F

C_D flow coefficient, A_M/A_{PM}

D_T capillary tube inside diameter, ft.

G_R reducer pressure gain

G_P amplifier pressure gain per stage

G_D dynamic pressure ratio (see eq. A8)

L_T capillary tube length, ft.

46

N_T	number of capillary tubes
N_S	number of amplifier stages
$P_G, P_{G1}, P_{G2}, P_{G3}$	garment circuit pressure, psf (see fig. 16)
P_{C1}, P_{C2}	mixing valve control pressure, psf
P_{C11}, P_{C12}	amplifier control pressures, psf
P_{CR1}, P_{CR2}	control pressures generated by bridge, psf
P_{DM}	mixing valve jet dynamic pressure, psf
P_{D1}	amplifier jet dynamic pressure, psf
P_C	cold water supply pressure, psf
P_H	warm water supply pressure, psf
P_{01}, P_{02}	mixing valve outlet pressure, psf
q	garment cooling rate, Btu/sec.
Q_C	cold water flow rate, ft^3/sec.
Q_{C1}	amplifier control port flow rate, ft^3/sec
Q_G	total flow through garment circuit, ft^3/sec.
Q_{G1}	flow through garment, ft^3/sec.
Q_H	warm water flow rate, ft^3/sec.
$Q_{HR}, Q_{HG}, Q_{CR}, Q_{CG}$	flow rates within mixing valve, ft^3/sec.
R_C	ratio of control port area to power port area
R_2	bridge circuit resistances

T_H	warm supply temperature, °F
T_G	garment inlet temperature, °F
T_C	cold supply temperature, °F
$\bar{T}_S$	mean skin temperature, °F
U	garment heat transfer coefficient, Btu/ft^2 °F sec.
α, β	constants in garment pressure drop equation
γ	flow ratio Q_G/Q_{G1}
λ	$(T_H - T_G) / (T_H - T_C)$
ξ	$UA_S / \rho c Q_{G1}$
μ	viscosity, lb sec/ft^2
ρ	density, slugs/ft^3

REFERENCES

1. Starr, J. B.; and Merrill, G. L.: Fl $\cdot$ ic Temperature Control for Liquid-Cooled Flight Suits. Report No. NA $\cup$ C-AC-6818, Naval Air Development Center, Johnsville, Pa.

2. Eckert, E. R. G.; and Drake, R. M.: Heat and Mass Transfer, Second ed., Chp. 17, McGraw-Hill Book Co., Inc. 1959.